

International Atomic Energy Agency

INDC(CCP)-367

Distr.: L

INDC

INTERNATIONAL NUCLEAR DATA COMMITTEE

**INTEGRAL TESTS OF NEUTRON NUCLEAR DATA
OF ACTINIDES**

(Translations of selected Russian papers published in Yadernye Konstanty 1987-1991)

Translation editor: Dr. A. Lorenz

February 1994

IAEA NUCLEAR DATA SECTION, WAGRAMERSTRASSE 5, A-1400 VIENNA

Reproduced by the IAEA in Austria
February 1994

**INTEGRAL TESTS OF NEUTRON NUCLEAR DATA
OF ACTINIDES**

(Translations of selected Russian papers published in Yadernye Konstanty 1987-1991)

Translation editor: Dr. A. Lorenz

February 1994

Table of Contents

	<u>Page</u>
Checking of Neutron Data for a Number of Actinides in Integral Experiments	1
S.M. Bednyakov, V.A. Dulin, I.V. Malysheva, G.N. Manturov, A.M. Tsibulya (Russian original in Yadernye Konstanty 4/1991, p. 71-84)	
Test of the Temperature Dependence of ^{238}U Cross-Section Structure in the Unresolved Resonance Region Using Transmission Experiments	17
V.N. Koshcheev, E.V. Dolgov, M.N. Nikolaev, V.V. Sinitsa, A.M. Tsibulya (Russian original in Yadernye Konstanty 1/1989, p. 73-81)	
On the Contradiction Between the Microscopic and Integral Data for Fast Neutron Absorption Cross- Section for ^{238}U Nuclei	31
A.A. Van'kov (Russian original in Yadernye Konstanty 1/1989, p. 90-93)	
The Effect of $\bar{\nu}(E)$ Energy Dependence at $E < 1$ eV on the Group Constants of ^{239}Pu in the Lower Energy Groups	39
A.G. Gusejnov, M.A. Gusejnov, N.S. Rabotnov (Russian original in Yadernye Konstanty 4/1988, p. 17-21)	
Testing of the ^{235}U , ^{238}U and ^{239}Pu Cross-Section Resonance Structure Data in the Unresolved Resonance Region Using Transmission Experiments	47
V.N. Koshcheev, E.V. Dolgov and A.M. Tsibulya (Russian original in Yadernye Konstanty 4/1988, p. 39-49)	
Testing of Cross-Section Functionals in the Unresolved Resonance Region	67
V.N. Koshcheev, A.S. Krivtsov, V.V. Sinitsa, V.F. Ukraintsev (Russian original in Yadernye Konstanty 4/1987, p. 73-80)	

Possible Influence of Correlation Between ν and Γ_f on
Resonance Shielding of $\bar{\nu}$ 81
A.G. Gusejnov, M.A. Gusejnov, N.S. Rabotnov
(Russian original in Yadernye Konstanty 4/1987, p. 38-43)

**CHECKING OF NEUTRON DATA FOR A NUMBER OF ACTINIDES
IN INTEGRAL EXPERIMENTS**

S.M. Bednyakov, V.A. Dulin, I.V. Malysheva,
G.N. Manturov, A.M. Tsibulya
Institute of Physics and Power Engineering, Obninsk

ABSTRACT

A comparison of calculational and experimental results of average cross-section and reactivity coefficient ratios for the actinides ^{237}Np , ^{239}Pu , ^{241}Am and ^{243}Am has been performed. Measurements have been performed in the spectra of various fast critical assemblies. The calculational results were obtained using the BNAB-90 evaluated data library. Conclusions regarding the reliability of actinide fission and capture cross-sections and the possibility to improve their accuracies is suggested.

INTRODUCTION

An increasing amount of attention is currently being focused on the problem of actinides contained in spent fuel from nuclear power plants. As is well known, the activity of the fuel for several hundreds and thousands of years after disposal is entirely determined by the activity of the actinide nuclides ^{237}Np , ^{238}Pu , ^{241}Am , ^{243}Am , ^{244}Cm and others which have accumulated in it. This makes it practically impossible to use this fuel and creates a considerable radiation risk in the area of spent fuel repositories. As it is now being discussed [1], this problem can be solved by recycling spent nuclear fuel in fast fission reactors, for example, by transmutation of the actinides into fission products with shorter half-lives.

In order to evaluate the half-life and recycling parameters, it is necessary to know the capture and fission cross-sections of the actinide nuclides over a wide range of neutron energies from ≈ 10 keV to several MeV.

In this work, we analyse the results of measurements of average fission cross-section and reactivity coefficients ratios obtained in experiments at fast critical assemblies. for the actinides ^{237}Np , ^{238}Pu , ^{241}Am and ^{243}Am . These data are compared with calculations using the BNAB-90 new group data system developed at the Institute of Physics and Power Engineering and we draw conclusions about the possibility of refining the capture and fission cross-sections for actinides.

MEASUREMENTS AT CRITICAL FACILITIES AND CALCULATIONAL RESULTS

The average fission cross-section ratios $\bar{\sigma}_1/\bar{\sigma}_s$ for uranium-235 and the ratios of reactivity coefficients R_1/R_0 for plutonium-239 were measured for the ^{237}Np , ^{238}Pu , ^{241}Am and ^{243}Am nuclides in fast critical assemblies with different spectrum softness [2 and 3]. As can be seen from the Table, which presents a summary of the available experimental data, the most comprehensive program for checking actinide cross-sections was implemented at the FCA testing facility (Japan). The experiments carried out at the FCA critical assemblies provide information both on fission cross-sections and on capture cross-sections over a wide neutron energy range from ≈ 10 keV to 10 MeV. The GODIVA, JEZEBEL and other hard spectrum facilities provide information only for fission cross-sections and only in the high-energy part of the spectrum. Experiments at other facilities supplement only the data for neptunium-237.

The calculations for all the critical assemblies were carried out in a single-dimension geometry in P_1 and S_n

approximations using the KRAB-1 program with ARAMAKO-80 data processing software based on BNAB-78 data [5]. The calculations of the measured cross-section and reactivity ratios were carried out using BNAB-90 data compiled on the basis of evaluated neutron data files [6].

Figures 1-5 show a comparison of the calculated and experimental data obtained at the critical assemblies. They also present the results of calculations using the JENDL-2 library (data taken from Ref. [3]). Correction for the effects of the heterogenous structure of critical assembly cells and the finite dimensions of the samples used in the measurements are made to the calculational results by applying the methods described in Refs [7 and 8].

DISCUSSION OF RESULTS

Figures 1-4 show a comparison of the ratios of the calculational and experimental results for measurements of $\bar{\sigma}_1/\bar{\sigma}_s$ and R_1/R_9 . As can be seen, for the fission cross-section ratios, the results obtained using the BNAB-90 data generally give a good description of all the experimental data. The discrepancies observed between calculation and experiment do not exceed an average of 3.5% for all the nuclides. The error caused by uncertainties in the fission cross-sections of the actinides is roughly the same. The calculated results for $\bar{\sigma}_1/\bar{\sigma}_s$ for all the actinides therefore do not contradict the expected values. The error in the experimental data is typically 2-2.5% and the cross-sections can be refined using the BNAB-90 data correction for experimental results at critical facilities.

Unlike to the average cross-sections ratios, in the case of the R_1/R_9 reactivity ratios there are significant discrepancies for all nuclides between the calculation and experimental results and it is difficult to explain such errors in the actinide constants. The experimental errors are $\approx 1-3\%$ but the results of

the calculations and the experiments frequently differ severalfold (in many cases the calculation and experiment values have different signs). Figure 5 shows the absolute values of the differences between the calculation and the experimental results. As can be seen, the observed dependencies of the C-E differences have a smoother character than the C/E ratio. Furthermore, as can be seen from the figures, the dependencies obtained using various BNAB-90 and JENDL-2 data are similar, with the C-E differences increasing as the share of neutrons below 40 keV increases. This fact can be explained, firstly, by the increase in the contribution of resonance neutrons to the reactivity R_1 for which capture cross-section resonance self-shielding factors constitute a large element of uncertainty (as can be seen from the data in Fig. 5, they need to be reduced considerably in the case of the BNAB data for ^{237}Np , ^{241}Am and ^{243}Am). Secondly, the increase in the share of soft neutrons in the spectrum poses higher experimental requirements. Thus the existing discrepancies in the soft critical assemblies can be explained partly by the presence of hydrogen impurities (for example in the form of water or oil) in the samples used to carry out the reactivity measurements. In general it should be noted that the results of the reactivity ratio measurements for the various critical assemblies are contradictory and it is difficult to use them to refine the capture cross-sections of the actinides studied. For this purpose we need to have more reliable experiments.

Figures 6-9 show the differential measurements of capture and fission cross-sections for the ^{237}Np , ^{238}Pu , ^{241}Am and ^{243}Am actinides and the group data obtained from various data libraries. The comparison shows that the cross-sections taken from the BNAB-90 data do not contradict the experimental results and the data from other libraries. It can also be seen that the capture cross-section differential measurements for the actinides do not enable us make it possible to assign an accuracy of more than 20-30% for the group cross-sections, and in the case of

^{238}Pu , the errors in the capture cross-sections are evidently 30-50%. According to our estimates, the errors in the average group fission cross-sections for the actinides are 5% (the data on the $\bar{\sigma}_1/\bar{\sigma}_3$ cross-section ratios do not contradict this).

CONCLUSIONS

From this analysis it follows that at present there is agreement between the macro and microscopic experiments on fission cross-section for the actinides ^{237}Np , ^{238}Pu , ^{241}Am and ^{243}Am and that the evaluated accuracy of the fission cross-sections for these actinides in the 0.5-10 MeV energy range is about 5-7%. The results of measurements of the reactivities of actinides does not give grounds for any hope of being able to refine the capture cross-sections. In order to do this, additional experiments must be carried out. The present level of accuracy of capture cross-sections for these actinides is 20-50%.

Summary of available experimental cross-section and reactivity coefficient ratio data for ^{237}Np , ^{239}Pu , ^{241}Am and ^{243}Am measured in critical assemblies

Assemblies	Fraction of neutrons below 40 keV in %	^{237}Np		^{238}Pu		^{241}Am		^{243}Am	
		$\bar{\sigma}/\bar{\sigma}_S$	R/R_0	$\bar{\sigma}/\bar{\sigma}_S$	R/R_0	$\bar{\sigma}/\bar{\sigma}_S$	R/R_0	$\bar{\sigma}/\bar{\sigma}_S$	R/R_0
FCA-IX-1	33,0	+	+	+	+	+	+	+	+
FCA-IX-2	23,0	+	+	+	+	+	+	+	+
FCA-IX-3	17,0	+	+	+	+	+	+	+	+
FCA-IX-4	7,1	+	+	+	+	+	+	+	+
FCA-IX-5	5,0	+	+	+	+	+	+	+	+
FCA-IX-6	4,3	+	+	+	+	+	+	+	+
FCA-IX-7	4,0	+	+	+	+	+	+	+	+
GODIVA	1,3	+							
JEZEBEL	1,0	+	+				+		
JEZEBEL-PU	1,0	+							
FLATTOP-25	1,6	+	+		+		+		
BIG-TEN	5,2	+	+		+				
ZPR-3-11	5,5	+							
ZEBRA-2	25,0	+							
ZEBRA-3	5,3	+							
VERA-11A	12,0	+							
VERA-1B	15,0	+	+						

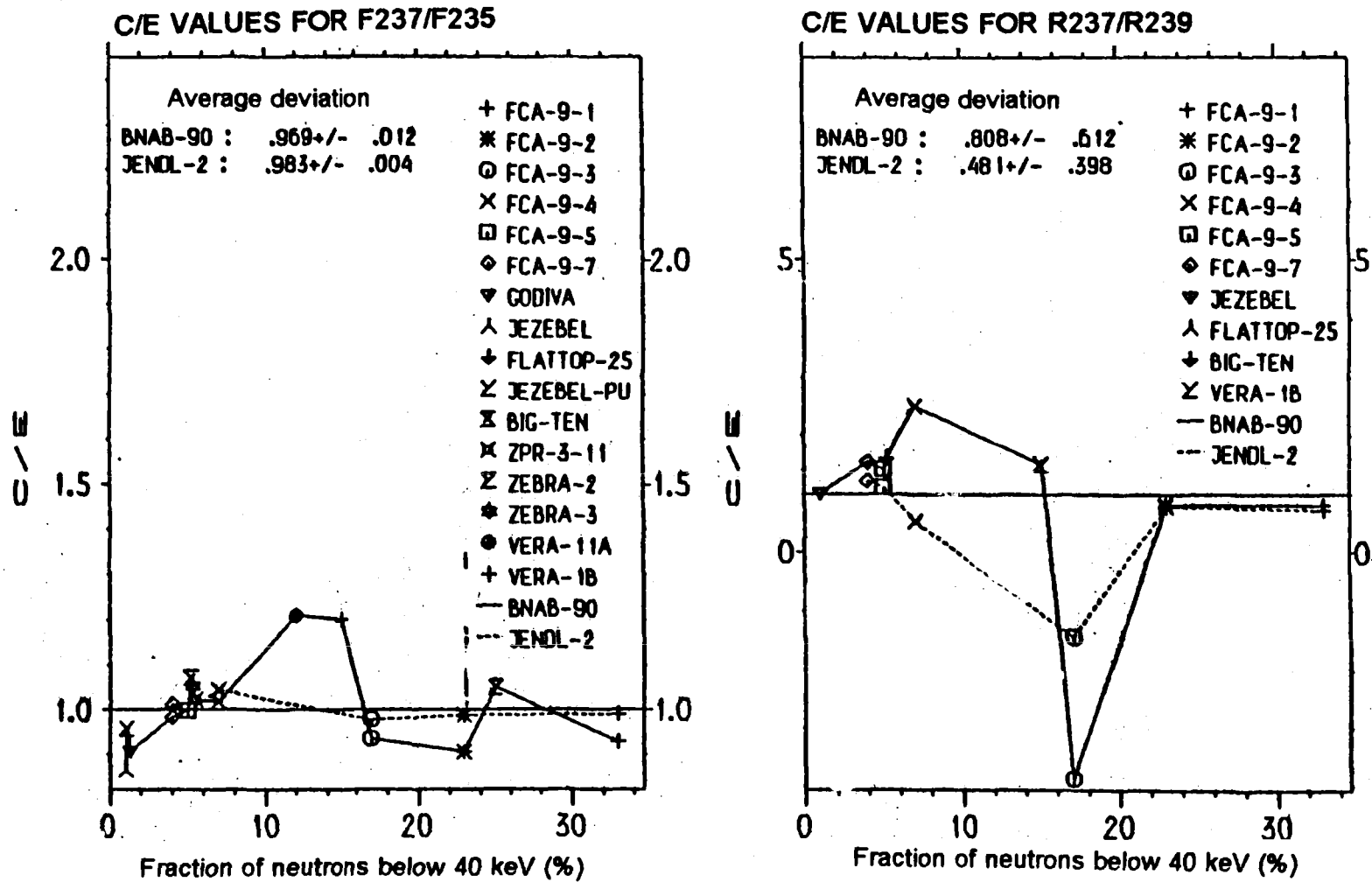


Fig.1 Comparison of integral data with experimental data for neptunium-237

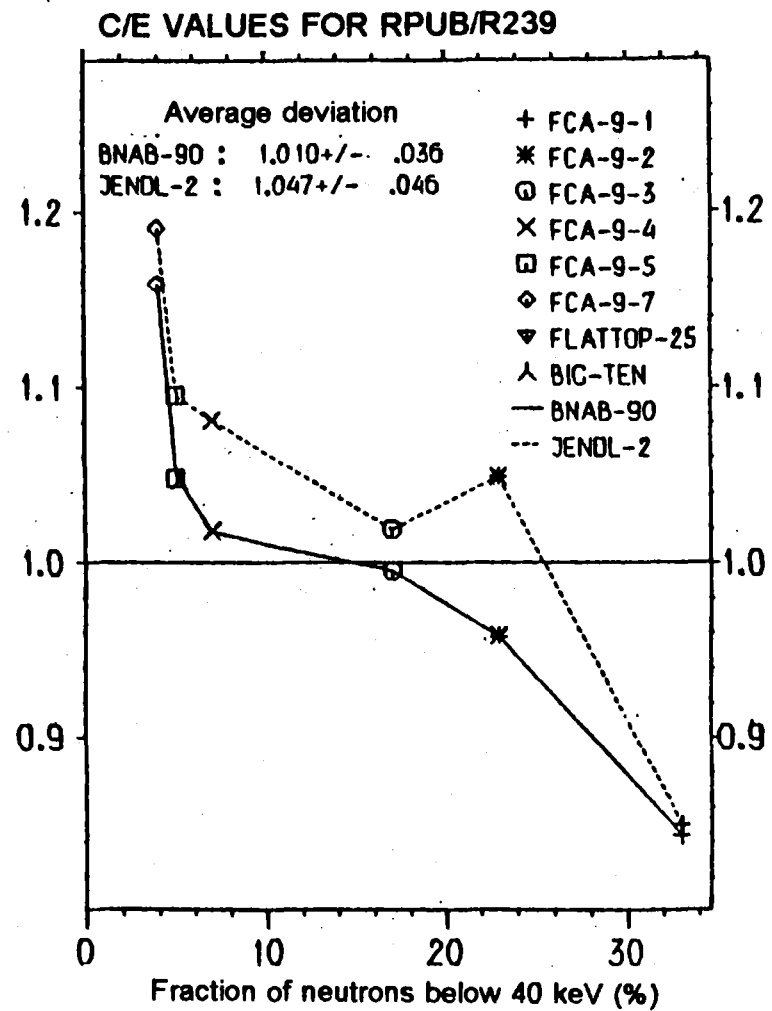
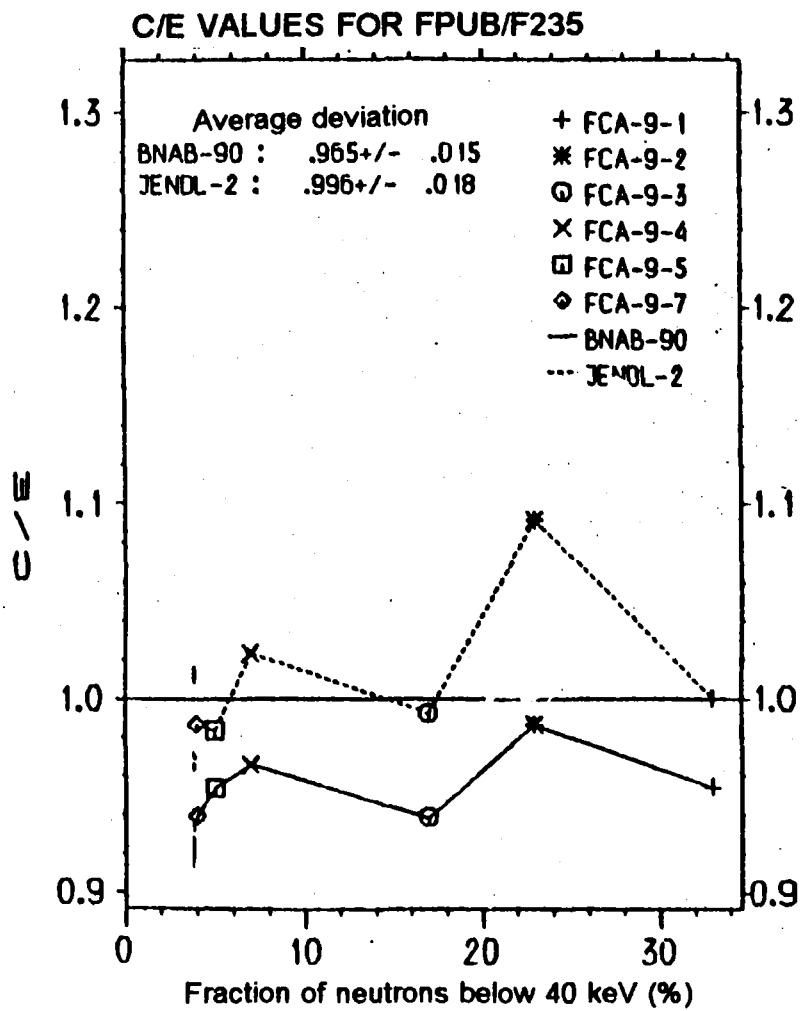


Fig.2. Comparison of integral data with experimental data for plutonium-238

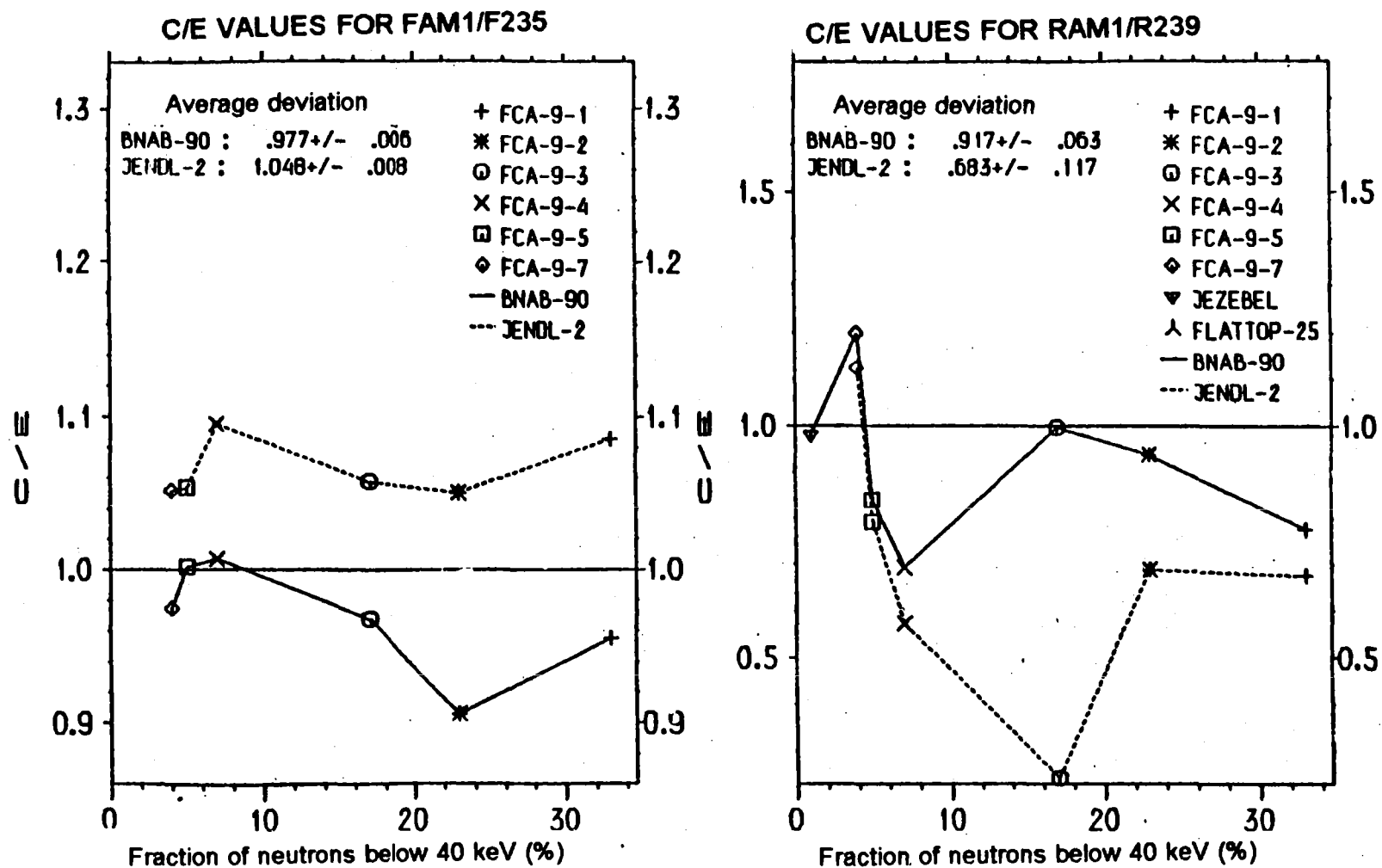


Fig. 3. Comparison of integral data with experimental data for americium-241

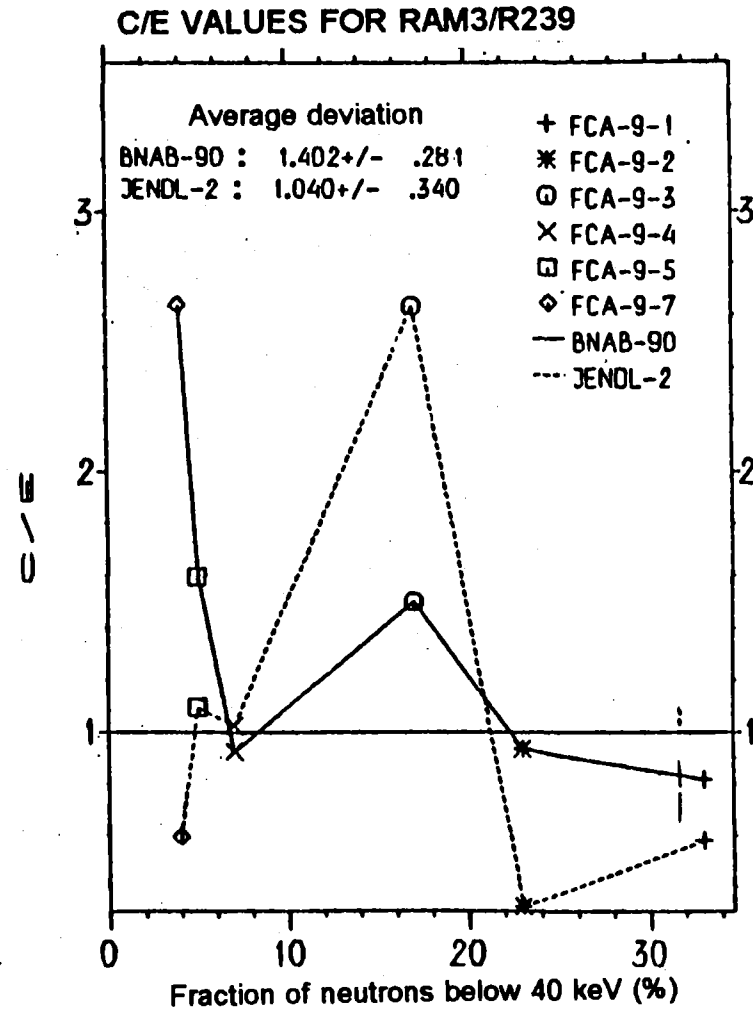
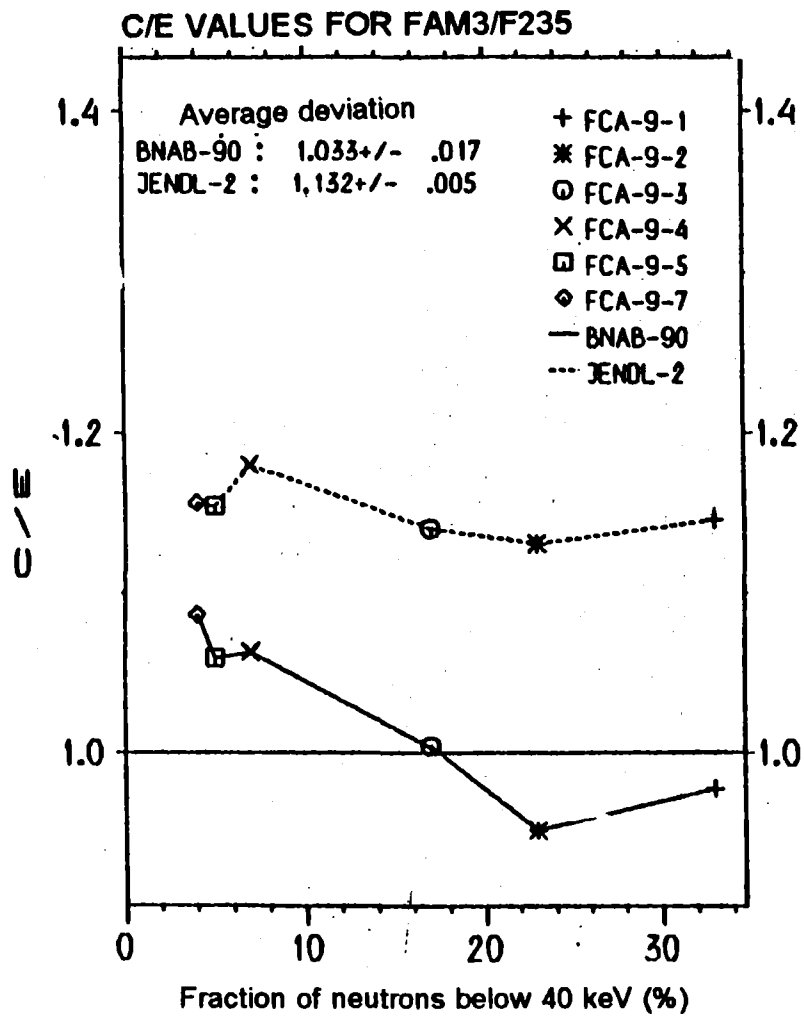


Fig. 4. Comparison of integral data with experimental data for americium-243

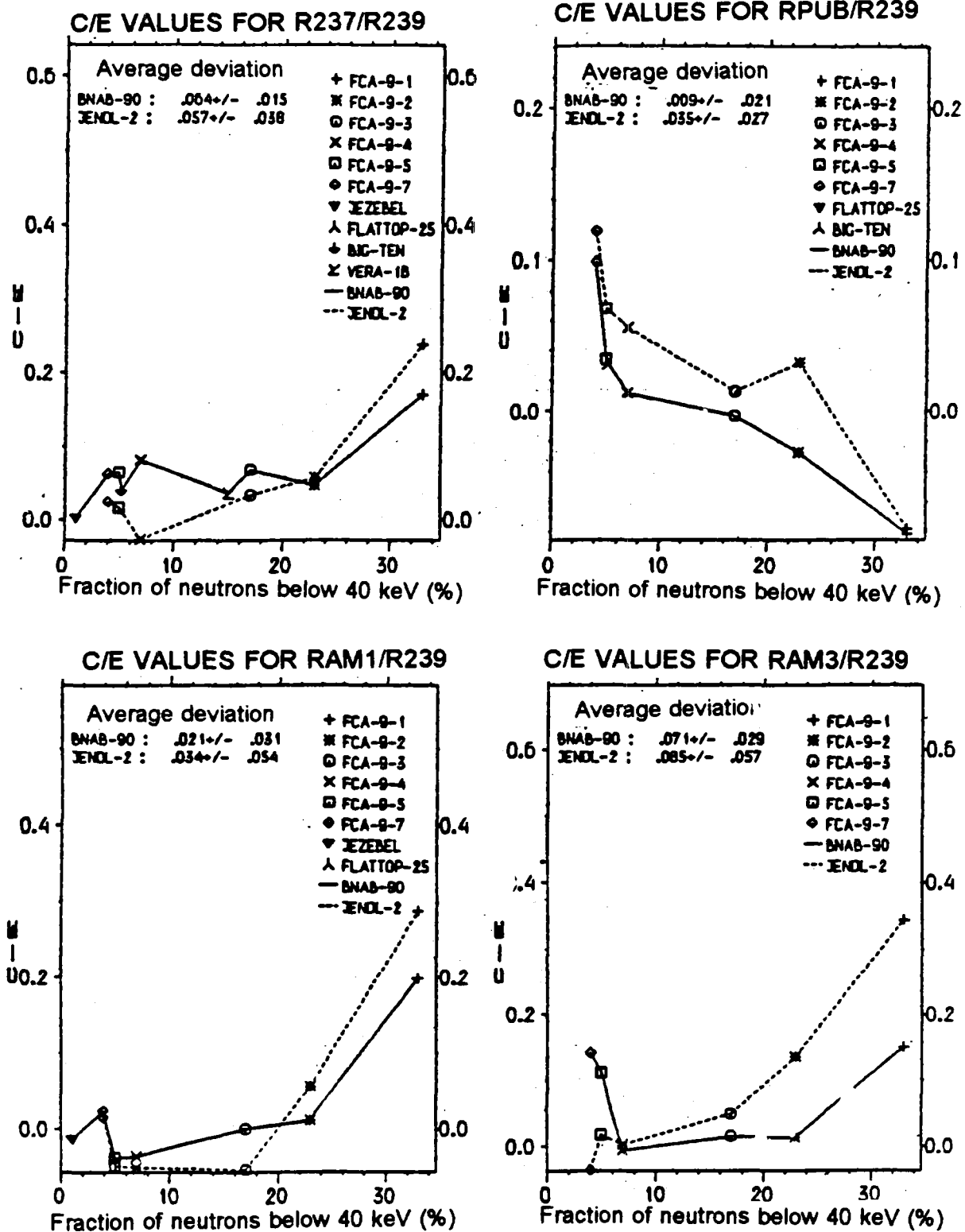


Fig. 5. Absolute values of the differences between measured and calculated reactivity data

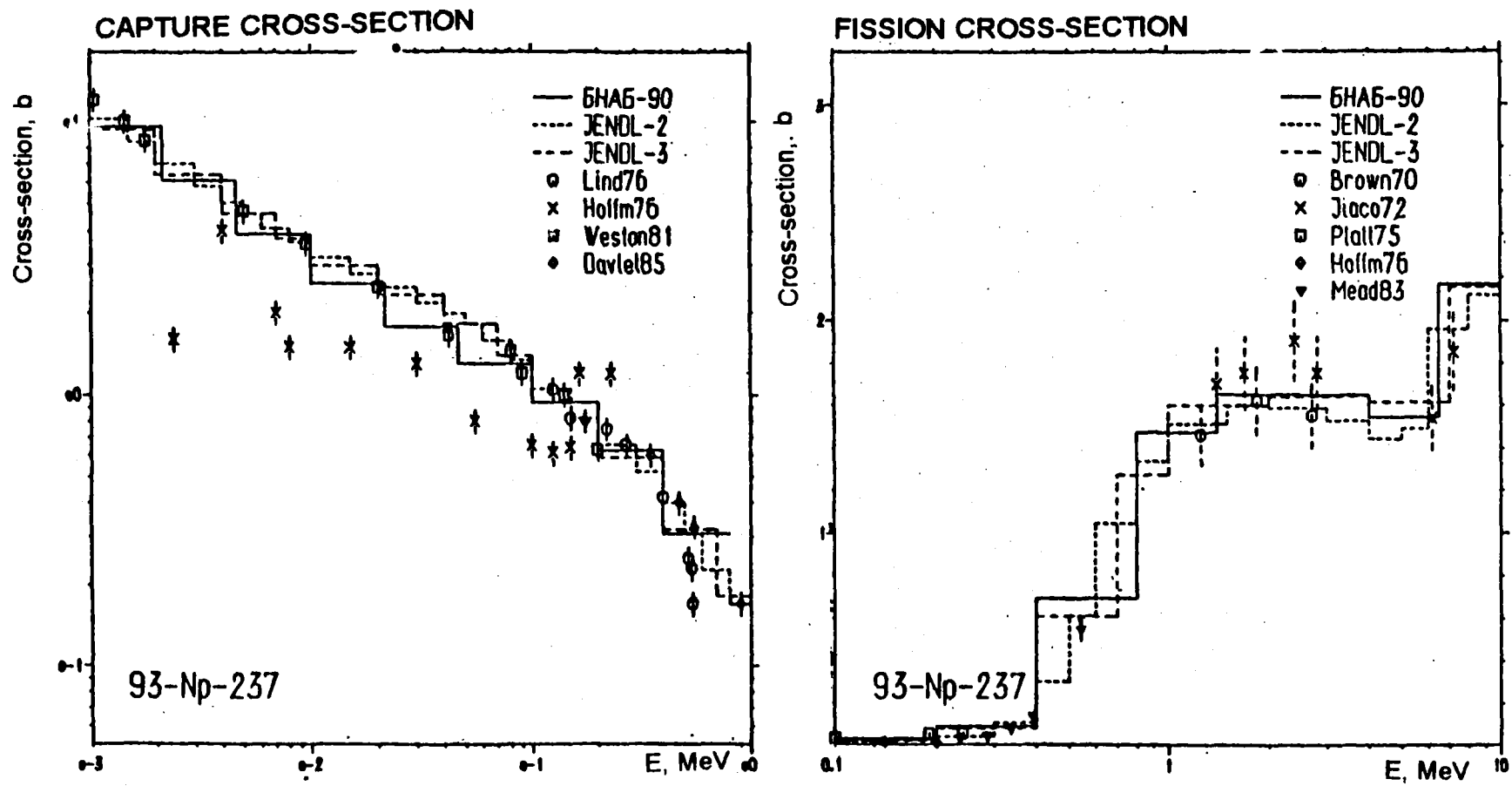


Fig. 6. Neptunium-237 capture and fission cross-sections

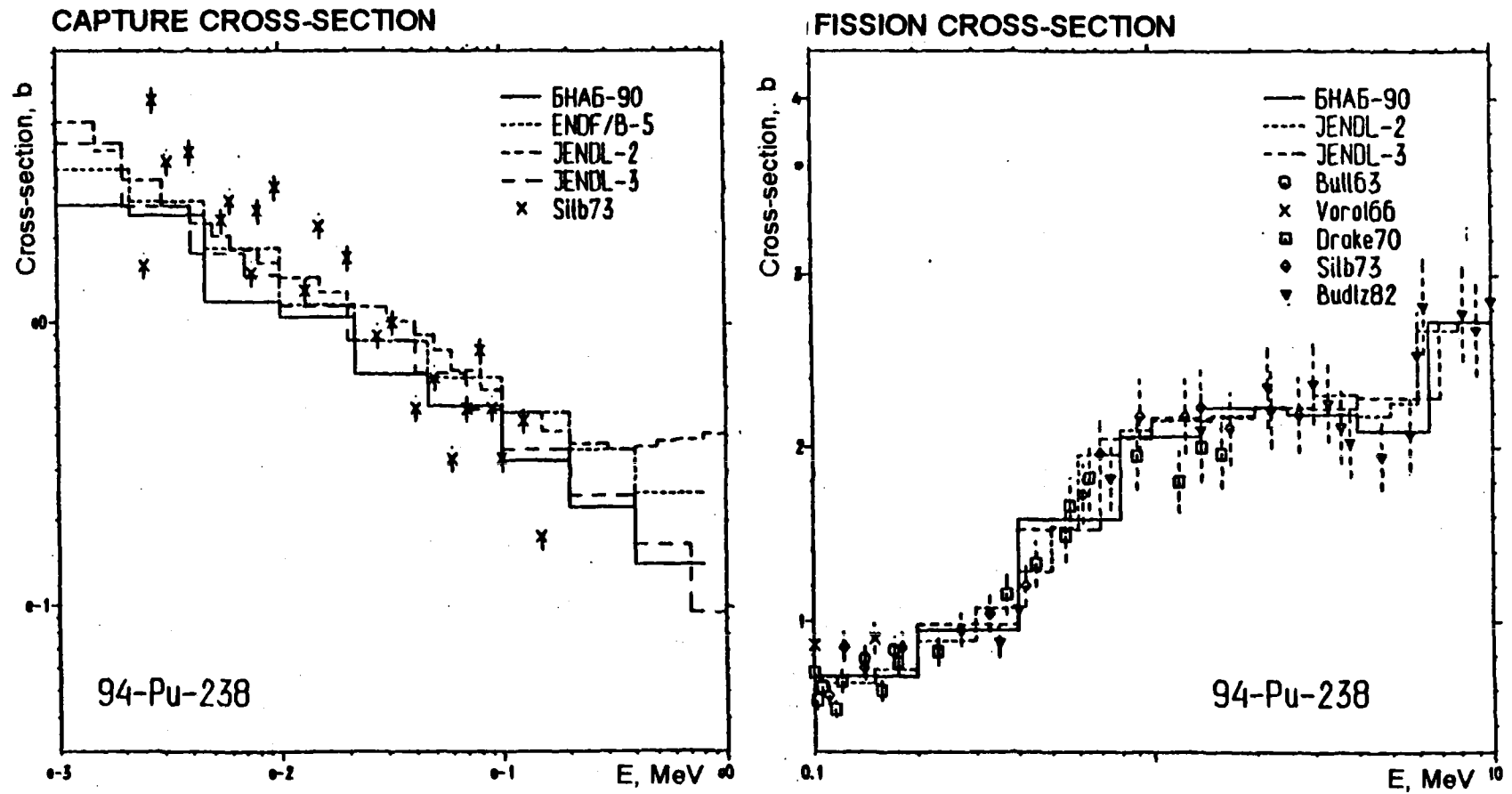


Fig. 7. Plutonium-238 capture and fission cross-sections

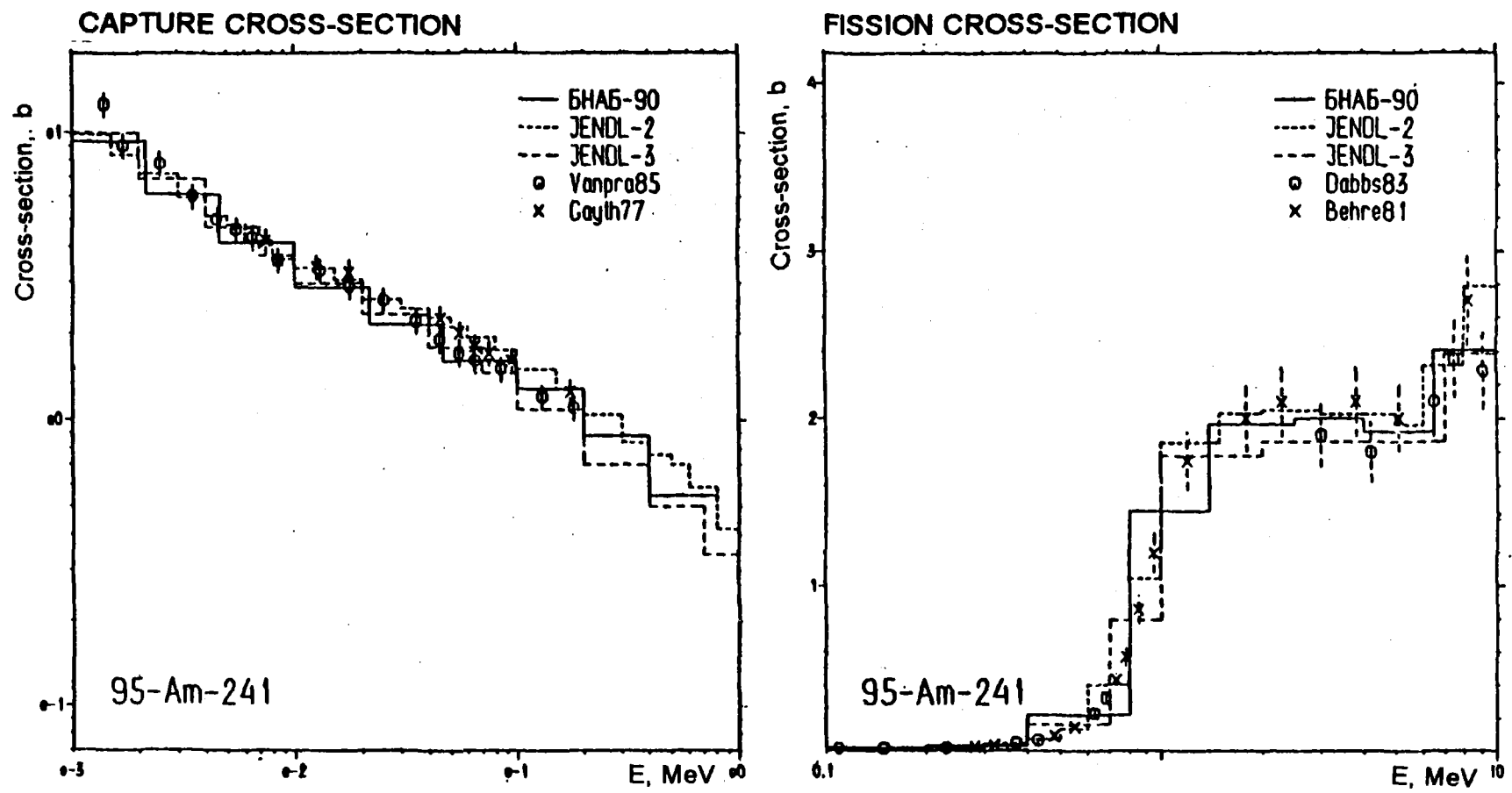


Fig. 8. Americium-241 capture and fission cross-sections

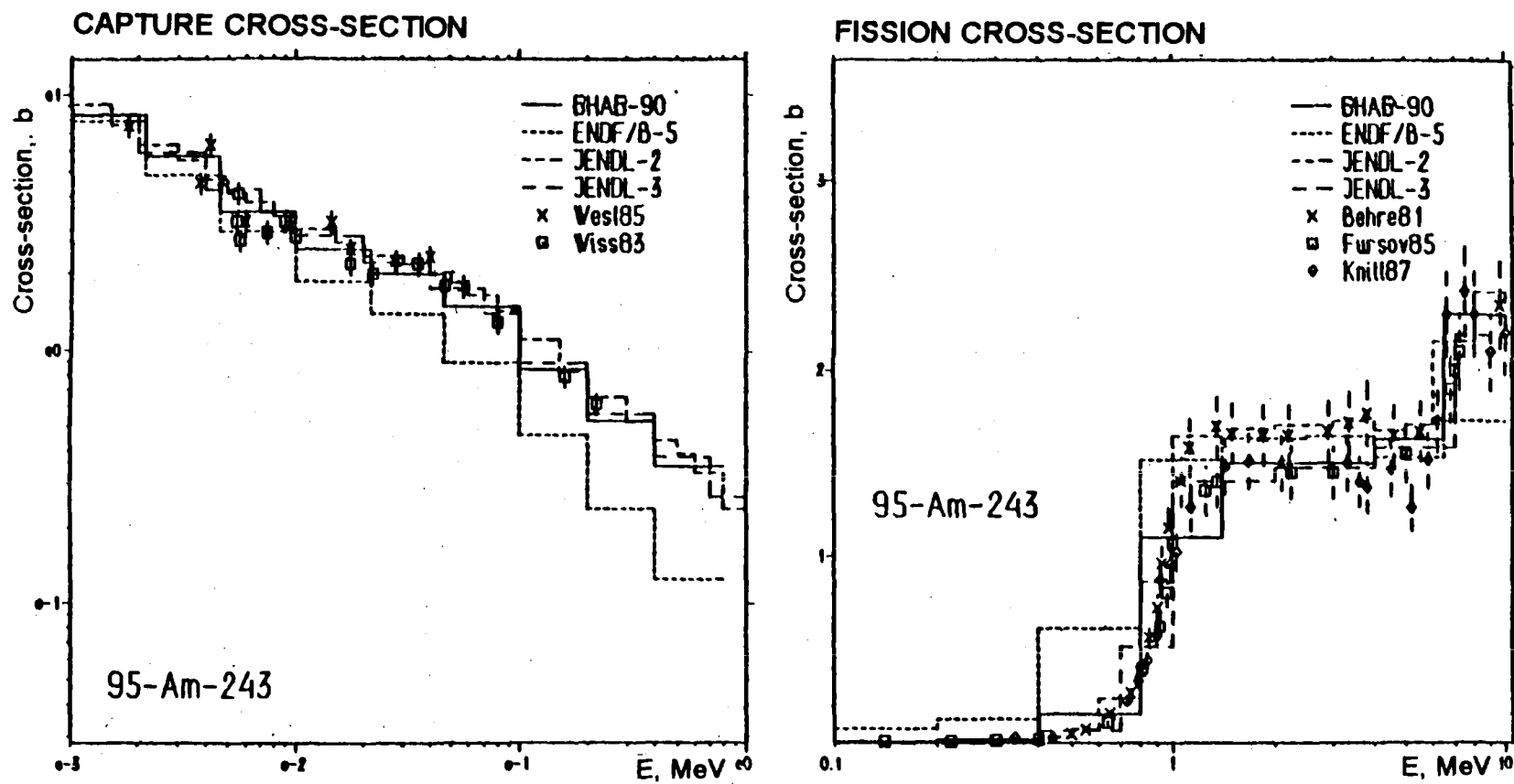


Fig. 9. Americium-243 capture and fission cross-sections

REFERENCES

- [1] First OECD/NEA Information Exchange Meeting on Separation and Transmutation of Actinides and Fission Products, Mito, Japan (1990).
- [2] "CSEWG benchmark specifications", Report BNL-19302, (1974).
- [3] MUKAYAMA, T., et al., Radiation Effects 93 (1986)147.
- [4] SAVOS'KIN, M.M., MOROZOVA, T.B., NOVIKOVSKAYA, E.I., et al., Voprossy atomnoy nauki i tekhniki, Ser. Fizika i tekhnika yadernykh reaktorov 6 43 (1984) 44 [in Russian].
- [5] ABAGYAN, L.P., BAZAYANTS, N.O., NIKOLAEV, M.N., TSIBULYA, A.M., Group Constants for Reactor and Shielding Calculations, Moscow, Ehnergizdat (1981) [in Russian].
- [6] BLOKHIN, A.I., et al., Conf.Proc. Nuclear Data for Science and Technology, Mito, Japan (1988) 611.
- [7] BEDNYAKOV, S.M., "Implementation of a method for evaluating integral experiments at the BSF testing facility", Preprint FEhI-2114, Obninsk (1990) [in Russian].
- [8] DULIN, V.A., At.Ehnerg. 66 (1989) 79 [in Russian].

Submitted for publication 7 May 1991

**TEST OF THE TEMPERATURE DEPENDENCE OF ^{238}U CROSS-SECTION
STRUCTURE IN THE UNRESOLVED RESONANCE REGION
USING TRANSMISSION EXPERIMENTS**

V.N. Koshcheev, E.V. Dolgov, M.N. Nikolaev,
V.V. Sinitisa, A.M. Tsibulya

ABSTRACT

Calculated ^{238}U transmission and self-indication functions and their temperature dependence in the unresolved resonance region are compared with experimental data in order to test the resonance structure parameters. The averaged resonance parameters from the FOND and ENDF/B-4 data libraries and the subgroup parameters from the MULTIC multi-group library have been used in this exercise.

Ref. [1] presented results of an evaluation of subgroup parameters for ^{238}U in the unresolved resonance region with temperature independent subgroup parameters. These subgroup parameters made it possible to describe fairly accurately the dependences of cross-section resonance self-shielding factors on the dilution cross-section and the temperature. However, the question of the accuracy of the self-shielding factors themselves and their temperature sensitivity remain open. The self-shielding factors assumed in [1] were calculated on the basis of average resonance parameters. Having evaluated how accurate our knowledge of these parameters is, and having calculated the sensitivity coefficients of the self-shielding factors for them, it is certainly possible to evaluate the accuracy of the self-shielding factors as well, but only in the context of an accepted parametric model of cross-section structure in the unresolved resonance region. The reliability of such an evaluation is somewhat questionable.

It is therefore of great importance to test the accepted data for the cross-section structure in the unresolved resonance region using experimental data which are directly sensitive to that structure. Such is the case with the transmission functions measured in circumstances where the geometry is "good". In [2] are given the results from testing the accepted parameters for ^{238}U cross-section structure in the unresolved resonance region using on the transmission function data obtained by various authors at a room temperature of $\theta_0 \sim 300$ K. On the whole, the testing confirmed the accuracy of those cross-section structure descriptions generated by the extrapolation of cross-section resonance structure characteristics for the unresolved resonance region and by theoretical description of the energy dependence of the average cross-sections in the unresolved resonance region itself.

This paper describes the results from testing of the temperature dependence of the ^{238}U cross-section resonance structure parameters (the subgroup parameters from [1] and the average resonance parameters from the ENDF/B-IV and FOND libraries) in the unresolved resonance region using transmission experiments.

Review of experimental data

Total and capture transmission functions can be determined for a given sample temperature θ and thickness $n(\theta)$ by means of an experiment consisting of the transmission of a neutron beam through the measured sample. For the total transmission function:

$$T_t(\theta, n(\theta)) = \int \psi(E) e^{-n(\theta) \sigma_t(\theta, E)} dE / \int \psi(E) dE;$$

and the capture transmission function:

$$T_c(\theta, n(\theta), \theta_0) = \int \psi(E) \tilde{\sigma}_c(\theta, E) e^{-n(\theta) \sigma_t(\theta, E)} dE / \int \psi(E) \tilde{\sigma}_c(\theta, E) dE,$$

where $\varphi(E)$ is the neutron flux spectrum; $\sigma_t(\theta, E)$ and $n(\theta)$ are the total cross-section and the thickness of the sample at temperature θ and $\sigma_c(\theta_0, E)$ is the capture cross-section of the detector at temperature θ_0 . (as a rule $\theta_0 \sim 300$ K).

Observed cross-sections calculated using the following formulae are often used as experimental data

$$\sigma_{\text{obs}}^t = -(1/n) \ln T_t \qquad \sigma_{\text{obs}}^c = -(1/n) \ln T_c$$

We should emphasize that both of these values represent valid interaction cross-sections: the difference is that $\sigma_{\text{obs}}(\text{total})$ is averaged over the resolution function $\varphi(E)$ uniformly over the energy range, whereas $\sigma_{\text{obs}}(\text{cap})$ is weighted by the capture cross-section $\sigma_c(\theta_0, E)$.

At the present time there exists a small body of experiments in which the temperature of the transmission function has been investigated for ^{238}U samples in the unresolved resonance region. They include the following:

- Van'kova A.A., Grigor'eva P.V., et al. [3], which describes the results of total transmission function measurement, averaged in the energy groups of the BNAB grouping for temperatures of $\theta = 77$ K, 293 K and 1043 K and for sample thicknesses of $n_0 = 0.0378$ at/b, 0.0575 at/b, 0.151 at/b and 0.303 at/b;
- Byoun T.Y et al. [4], which gives total $T_t(\theta, n(\theta))$ and capture $T_c(\theta, n(\theta))$ transmission functions at narrow energy intervals in the energy range from ~ 4.5 keV to ~ 90 keV for three temperatures $\theta = 101$ K, 300 K and 975 K, and two sample thicknesses 0.0316 and 0.0621 at/b;
- Tsang F. and Brugger R. [5], whose work gives highly detailed experimental information on the temperature dependence of the total observed cross-section in the temperature range from 100 K to 1100 K, at an energy of 24 ± 0.9 keV for four sample thicknesses = 0.0437; 0.0874; 0.1310 and 0.1747 at/b and at energy point $E = 144 \pm 12$ keV for two thicknesses = 0.0437 and 0.0874 at/b;

- Haste T. and Sowerby M. [6]. The only experimental information in this paper that was available to us was the data for the energy range of 3 to 4 keV which are given in the graph in Reference [7].

Calculational Models and Comparative Quantities

For the calculation we employed, firstly, the evaluated average resonance parameters for ^{238}U from the FOND and ENDF/b-4 libraries, and secondly the subgroup parameters from a preliminary version of the MULTIC [8] group data.

The first calculation was carried out using the GRUKON application package [9]. The main model characteristics assumed were as follows:

- the cross-section calculation was carried out using the single-level Breit-Wigner formalism in which the Doppler broadening effect was taken into account by means of the resonance form functions ϕ and χ ;
- neutron width fluctuations (including those in the inelastic scattering channel) were described by the Porter-Thomas distribution, the radiation width and level spacings fluctuations being disregarded.

The integrals for the resonance width distribution were calculated using quadrature formulae of the highest algebraic accuracy. A more complete description of this method is given in reference [10].

In the second instance the comparative quantities were calculated using subgroup parameters whose temperature dependence was determined by interpolation (or extrapolation) of the subgroup cross-sections on a logarithmic temperature scale.

In order to be able to observe "pure" temperature effects, a comparison was made between the experimental and calculational values of normalized transmission functions. For total transmissions the normalized transmission was determined by using the following equation:

$$R_t(\theta, n(\theta), \theta_0) = T_t(\theta, n(\theta)) / T_t(\theta_0, n_0).$$

A similar evaluation was made for total observed cross-sections:

$$R_t(\theta, n(\theta)) = \sigma_{obs}^t(\theta, n(\theta)) / \sigma_{obs}^t(\theta_0, 0)$$

where $\sigma_{obs}(\theta_0, 0)$ is the total observed cross-section extrapolated to zero-sample thickness.

As for the capture transmissions, these were compared using functions of the type

$$R_c(\theta, n(\theta), \theta_0) = \frac{T_c(\theta, n(\theta), \theta_0)}{T_c(\theta_0, n_0, \theta_0)} / R_t(\theta, n(\theta), \theta_0).$$

The temperature dependence of this coefficient shows the extent to which the temperature dependence of a capture transmission differs from that of a total transmission. Comparison with the experimental value of this quantity seems to give a better understanding of how accurately the calculation describes total cross-section temperature dependence in the vicinity of absorption resonances, than does a straightforward analysis of the coefficient:

$$T_c(\theta, n(\theta), \theta_0) / T_c(\theta_0, n_0, \theta_0).$$

One of the important aspects of these calculations was to account for changes in the density of the sample with temperature. We used the experimentally corroborated calculation curve cited in [5] for surface density changes in metallic uranium samples. This curve corresponds to the linear temperature expansion law.

The Doppler broadening calculations for resonances were conducted for an effective temperature θ , which in the case of metallic uranium differed noticeably from the sample temperature only at temperatures below 300K: $\theta_{\text{eff}}(77\text{K})=101\text{K}$.

Analysis of results

Figs. 1 and 2 show the results obtained from the comparison of normalized transmission functions $R_t(\theta, n(\theta), \theta_0)$ for various sample thicknesses when heated up to a temperature of 1000K. Similar results from a comparison of normalized transmission functions $R_t(\theta, n(\theta), \theta_0)$, but for temperatures of approximately 100K, are given in figs. 3 and 4. On the whole, good agreement can be observed between calculational and experimental values for the wide range of sample thicknesses considered.

The following should be noted:

- at greater thicknesses the curve obtained from subgroup parameters begins to diverge from both the experimental data and calculations which conducted for average resonance parameters using the GRUKON application package. This mismatch occurred because in the evaluation of subgroup parameters more emphasis was placed on the description of the ^{238}U cross-section resonance structure for dilution cross-sections values ($\sigma \geq 10$ barns) [1]. The description of resonances minima was thus not accurate enough. The discrepancy could be eliminated by introducing one more subgroup to describe the resonance cross-section minima;

- To describe experiments using cooled samples having an effective temperature θ_{eff} instead of the temperature θ , was essential, especially at greater thicknesses:

- it would seem that the change in sample density as a function of temperature has not been accurately explained by Byoun T. et al. When a sample cools down its density should

increase by approximately 1%. This has only a slight adverse effect on thin samples, where flow attenuation is small, but it begins to become noticeable at a thickness of 0.0621 at/b. According to the data provided by Byoun et al., the density of their sample did not change on cooling. When a sample 0.0621 at/b thick was heated to 975K, its density, according to the data in reference [4], was reduced by ~2% whereas, if the temperature dependence curve for surface density of metallic uranium from reference [5] is used, the change ought to be ~3.5%. Clearly, if in our calculations we had assumed a density change of a given sample which agreed with that in reference [5] (i.e. ~3.5%), then the agreement between the experimental data of Byoun et al. and the calculational values would have improved;

- The experimental data of Tsang and Brugger for a heated sample - this time at 24keV, and for a cold sample - indicate a stronger cross-section structure temperature dependence than the data of other authors.

It should be noted, however, in the calculational description of the experimental data obtained by Tsang and Brugger we came up against other, perhaps more significant problems. In Fig.5, for example, we see the data obtained by these authors for the temperature dependence of a normalized observed cross-section at two energies, namely 24 and 144 KeV. The straight line drawn through these energy points were calculated by the authors using average resonance parameters (quite close to those assumed in ENDF/B-4 by means of the U3R program. The figure also shows temperature dependence curves for a normalized observed cross-section which we calculated using the GRUKON application package based on the average resonance parameters assumed in ENDF/B-4 and FOND, and also obtained using subgroup parameters. Clearly, both the character and magnitude of the temperature dependence we obtained are quite different from those in [5]. Using the average resonance parameters given by Tsang and Brugger in [5] produced results which were very close to those obtained on the basis of ENDF/B-4. There is thus

a contradiction here which seems unlikely to be resolved without additional information.

Processing of the experimental capture transmission function data of Byoun et al. (see Figs. 6 and 7) showing the energy dependences for the function $R_c(\theta, n(\theta), \theta_0)$, showed that for hot samples the calculations performed using average resonance parameters agreed fairly well with the experimental data, especially when the average resonance parameters from the FOND library are used. It is true that with an increase in sample thickness at energies below 10 keV, the calculational value of the quantity $R_c(\theta, n(\theta), \theta_0)$ appears to be overstated. In experiments with cold samples, that discrepancy shows up far more strongly. It illustrates that the temperature dependence of capture transmission in the region below 10 keV does not differ as much from that of total transmissions as should follow from the calculation. The reason for this discrepancy are also difficult to resolve without further experimental data.

As regards the description of the function $R_c(\theta, n(\theta), \theta_0)$ by means of subgroup parameters, the insufficiently accurate description of total cross-section minima noted earlier also appeared here. The effect of this inaccuracy compensates (sometimes overcompensates) for the error in the description of $R_c(\theta, n(\theta), \theta_0)$ by means of average resonance parameters.

Conclusions

Our analysis leads us to the following conclusions:

1. The existing experimental data for temperature dependence of total and capture transmissions on the whole confirm the assumption about the nature of temperature dependence of the ^{238}U cross-section structure in the unresolved resonance region.
2. Solutions are needed for the small discrepancy, which nevertheless exceeds estimated experimental errors, in the

temperature dependence of capture transmissions in the energy range below 10 keV (which is essentially an area of partly resolved resonances).

3. The experiment of Tsang and Brugger resulted in considerable qualitative and quantitative differences in transmission function temperature dependence compared to those we calculated. Just as great were the differences in the results which Tsang and Brugger obtained from their calculations for average resonance parameters using the U3R program. It is possible that the reason for the discrepancies is a misunderstanding on our part of certain features of the data given in [5].

4. Further experimental research into temperature dependence for total and, in particular, capture transmissions would be extremely useful. It would be particularly interesting to measure the the dependence of a capture transmission $R_c(\theta, n(\theta), \theta_0)$ for a sample/detector temperature θ_0 at a constant sample/filter temperature.

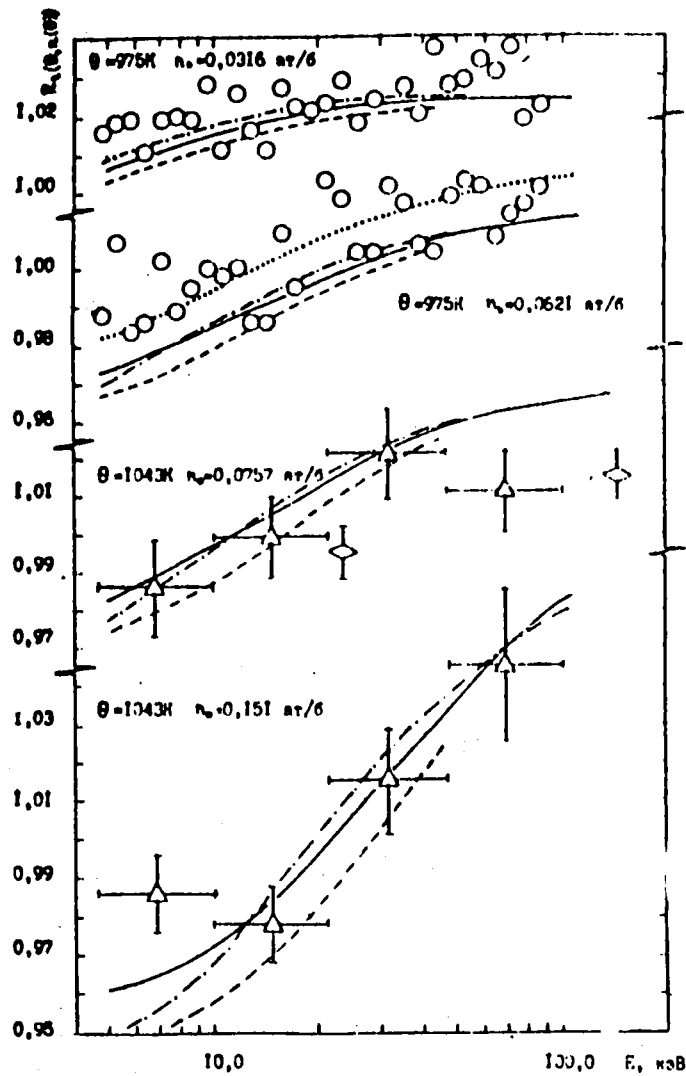


Fig. 1. Energy dependence of a normalized total transmission function for heated ^{238}U samples:
 $\circ = [4]$; $\blacktriangle = [3]$; $\diamond = [5]$;
 - - - ENDF/B-4; - - - - MULTIC;
 — FOND; FOND with sample density (75K) = 0.06 at/g.

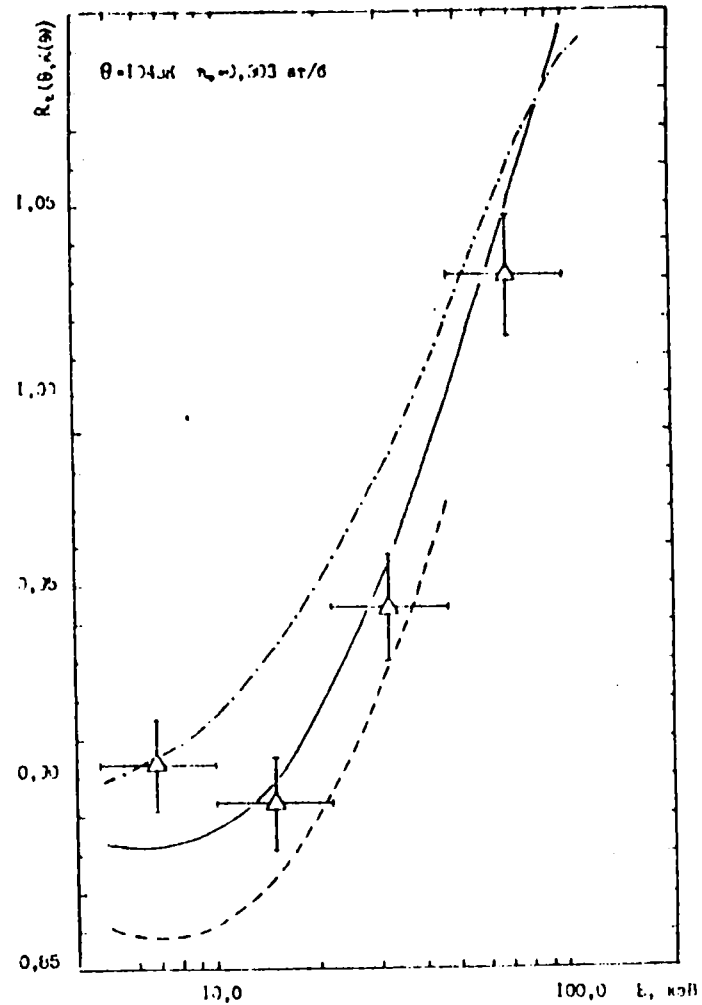


Fig. 2. Energy dependence of a normalized total transmission function for a heated ^{238}U sample: $\blacktriangle = [3]$; - - - ENDF/B-4; - - - - MULTIC; — FOND.

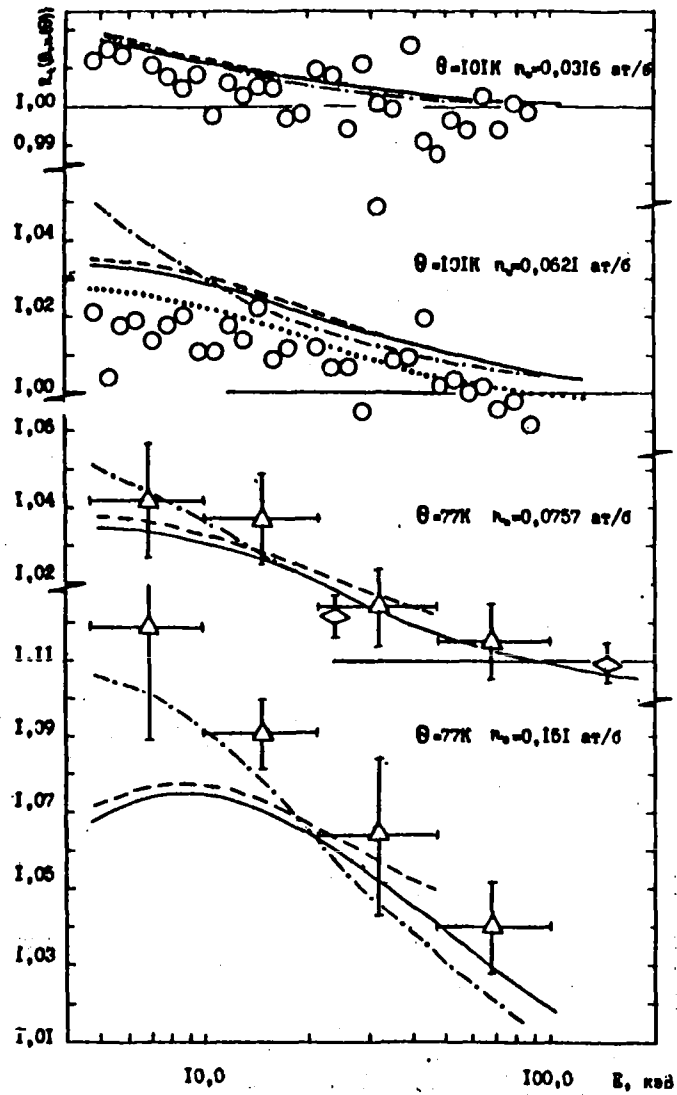


Fig. 3. Energy dependence of a normalized total transmission function for cooled ^{238}U samples: \circ = [4]; \blacktriangle = [3]; \diamond = [5]; ---- ENDF/B-4; -.-.- MULTIC; — FOND; FOND with sample density (101K) 0.0628 at/b.

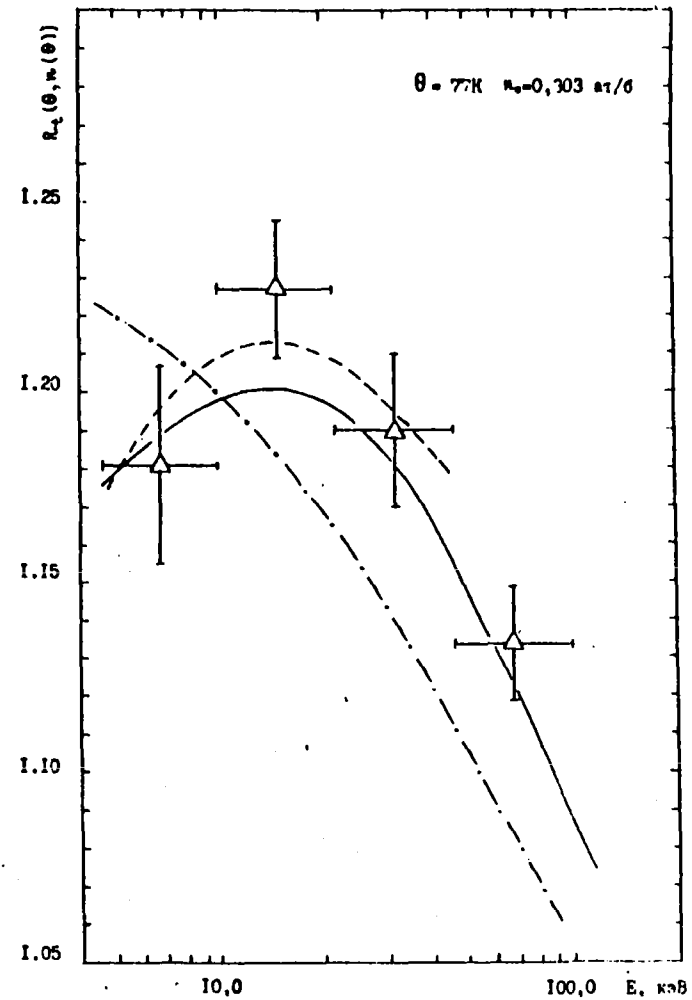


Fig. 4. Energy dependence of a normalized total transmission function for a cooled ^{238}U sample: \blacktriangle = [3]; ---- ENDF/B-4; -.-.- MULTIC; — FOND.

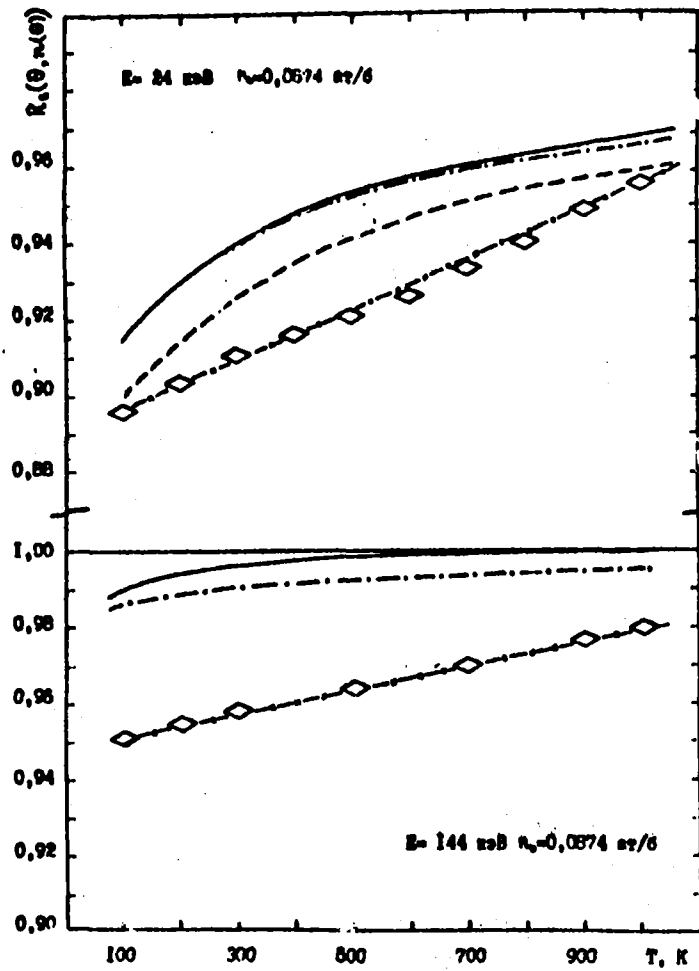


Fig. 5. Temperature dependence of a normalized observed cross-section for a ^{238}U sample; $\diamond = [5]$;
 - - - - MULTIC; ——— FOND;
 - - - - ENDF/B-4; - - - - U3R.

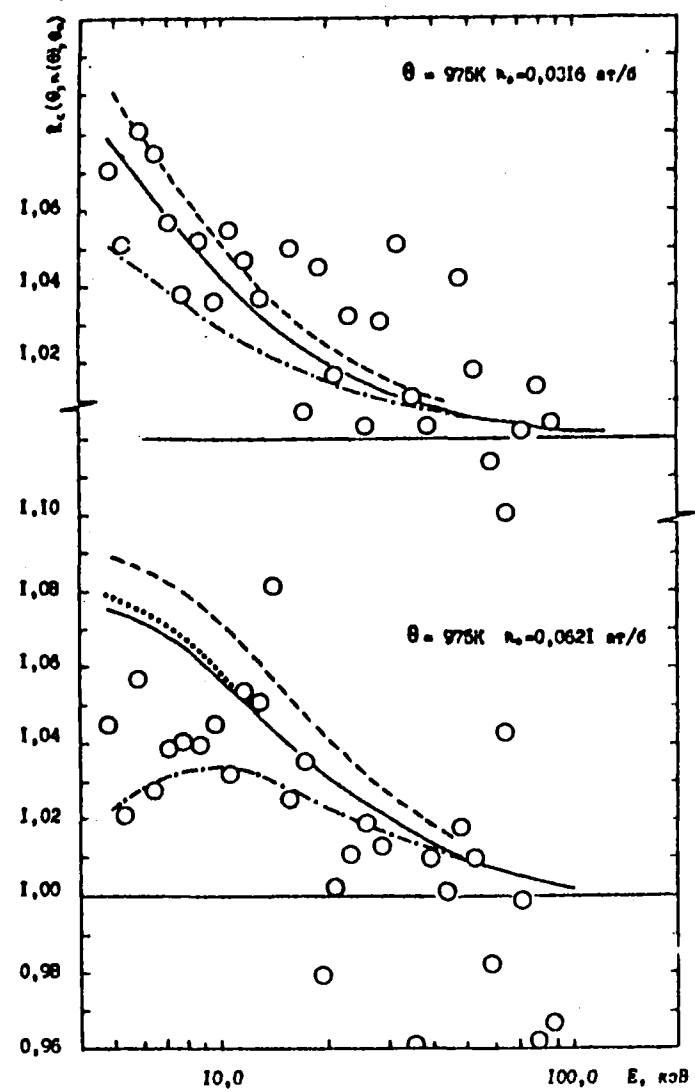


Fig. 6. Energy dependence function $R_n(\Theta, n(\Theta), \Theta_0)$ for heated ^{238}U samples; $\circ = [4]$; - - - - ENDF/B-4; - - - - MULTIC; ——— FOND; FOND with sample density (975K) 0.06 at/b.

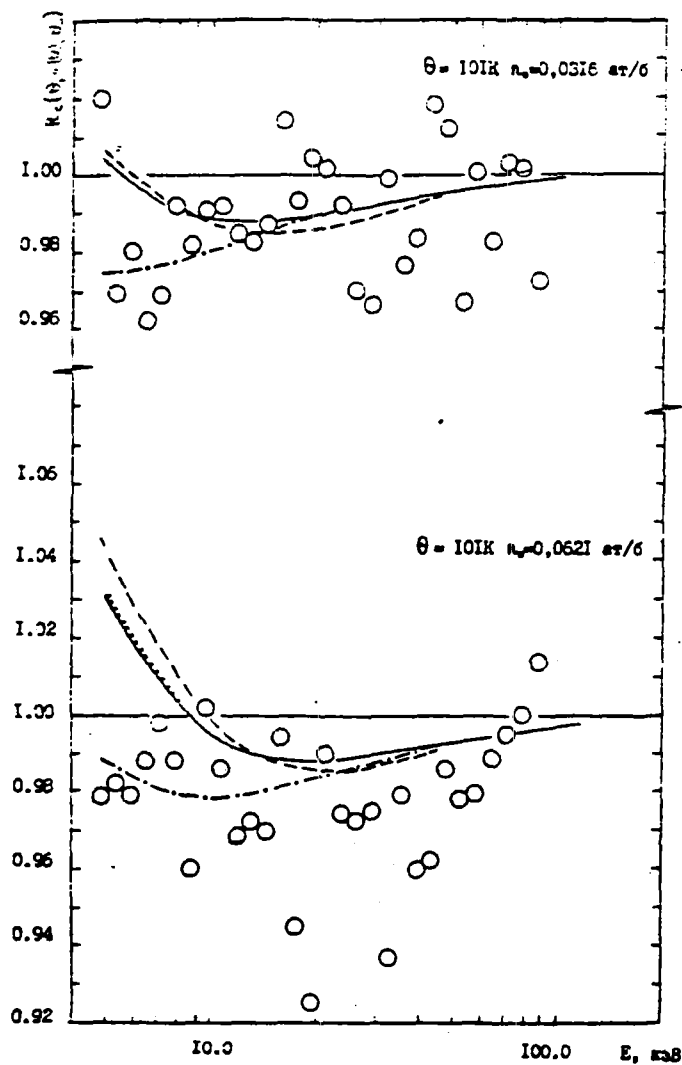


Fig. 7. Energy dependence of function $R_c(\theta, n(\theta), \theta_0)$ for cooled ^{238}U samples: \circ - [4]; ---- ENDF/B-4; -.-.- MULTIC; — FOND; FOND with sample density (101K) 0.0628 at/b.

REFERENCES

- [1] DOLGOV, E.V., KOSHCHEEV, V.N., SINITSA, V.V., Subgroup parametrization of the cross-section structure of basic fuel materials in the unresolved resonance range, in Proc. Int. Conf. on Neutron Physics, Kiev, 21-25 September 1985. [in Russian]
- [2] KOSHCHEEV, V.N., DOLGOV, E.V., TSIBULYA, A.M., Voprosy atomnoj nauki i tekhniki, Nucl. Const. 4 (1988) 39. [in Russian]
- [3] GRIGOR'EV, Yu.V., Measurement of neutron cross-sections and uranium-238 resonance characteristics on the spectrometer at the IBR reactor, Diss. (Abstract) Dubna (1980).
- [4] BYOUN, T.Y., et al., Temperature Dependent Neutron Transmission Measurements in ^{238}U , Proc. Nat. Topical Meeting on New Development in Reactor Physics and Shielding, 12-15 September, 1972, New York, USAEC, p.1115.
- [5] TSANG, F.Y., BRUGGER, R.M., Nucl. Sci. Eng. 72 (1979) 55.
- [6] HASTE, T.J., SOWERBY, M.G., Report AERE-R 8961, Harwell (1978).
- [7] BEE, N.J., The relationship between the local S-wave strength function in ^{238}U , in Proc. IAEA Cons. Mtg. on U and Pu Isotope Resonance Parameters, 28 Sep.-2 Oct. 1981, Vienna, (INDC(NDS)-129/GJ (1982) 182.
- [8] DOLGOV, E.V., SAVOS'KIN, M.M., TSIBULYA, A.M., Voprosy atomnoj nauki i tekhniki, Nuclear Constants 5(59) (1984) 49. [in Russian]
- [9] SINITSA, V.V., Voprosy atomnoj nauki i tekhniki, Nuclear Constants 5(59) (1984) 34. [in Russian]
- [10] SINITSA, V.V., Voprosy atomnoj nauki i tekhniki, Nuclear Constants 5(54) (1983) 3. [in Russian]

Submitted for publication 18 May 1988

**ON THE CONTRADICTION BETWEEN THE MICROSCOPIC AND
INTEGRAL DATA FOR FAST NEUTRON ABSORPTION
CROSS-SECTION FOR ^{236}U NUCLEI**

A.A. Van'kov

ABSTRACT

The contradiction between a measured integral neutron absorption cross-section averaged over a fast reactor spectrum and the corresponding value which was calculated with the use of evaluated microscopic cross-sections and a theoretical neutron spectrum has been investigated. The possible systematic error of a correction factor which takes into account multiple resonance neutron scattering in samples used in the measurement of the absorption cross-section is investigated. It is proposed that this error may be one of the main reason for the contradiction mentioned above which arises in the measurement of the ^{236}U neutron absorption cross-section.

Radiative capture cross-sections of heavy nuclei in the energy range of a few keV to ~ 0.5 MeV are usually measured using neutron time-of-flight spectrometers by recording the γ -quanta emitted during radiative capture of neutrons in a thin sample. For heavy nuclei, this energy range is the unresolved resonance region. Resonance effects are particularly pronounced at low energies and therefore the "optical" thickness of the sample increases as the energy of the incident neutrons decreases. A compromise has to be found between the contradictory requirements of collecting statistical data rapidly and of ensuring a minimum distortions of the observed cross-section caused by the effects of resonance self-shielding and absorption after scattering of the neutrons in a sample of finite thickness. In practice, samples having a thickness of about $x = 1$ mm, i.e. $t = 5 \cdot 10^{-3}$ nucl/b are used in such experiments. Such samples are far from being "ideally thin" since the relative correction for σ_γ for

scattering at $\sigma_s \sim 10$ b is of the order of $2\sigma_{s,t}$, i.e. 10% (if the mean path length is taken to be $2x$). If the contribution to the error of σ_T as a result of this correction were to be less than 1% this would mean that the scattering effect correction would have to be known within an error not worse than 10%.

In evaluating this correction, the main difficulty lies in correctly taking into account the resonance structure of the neutron cross-sections. With the existing approximation methods it was not possible to check if the resonance structure was taken into account correctly since there were no adequate mathematical methods for representing it on the basis of the theory of neutron cross-section behavior in the unresolved resonance region. We have developed a way of representing it based on the R-matrix theory using the Monte Carlo method to generate the total cross-section function and the partial cross-section correlation functions [1, 2]. It thus became possible to calculate reliably any non-linear cross-section behavior. Adopting this approach, the author developed an analytical method of calculating the correction for multiple scattering of neutrons in the sample, taking into account the resonance structure of the neutron cross-sections.

Let us examine the essence of our calculational method, the geometry of which is shown in Fig. 1. The symbols used are as follows:

- | | | |
|------------------------------|------------------|--|
| σ' | $= \sigma(E')$ | - total cross-section; |
| σ'_T | $= \sigma_T(E')$ | - absorption cross-section; |
| σ'_s | $= \sigma_s(E')$ | - scattering cross-section; |
| $\sigma, \sigma_T, \sigma_s$ | | - corresponding cross-sections at energies E after initial scattering; |
| x | | - thickness of layer, cm; |
| n | | - density of nuclei, cm^{-3} ; |
| t = nx | | - thickness of the layer, nucl/b; |
| $\mu = \cos\theta$ | | - cosine of the scattering angle of . |

The observed self-shielding cross-section which is proportional to the number of absorption events at the first collision in a layer of thickness t is

$$\langle \tilde{\sigma}_r \rangle = \frac{1}{t} \langle (1 - e^{-\tilde{\sigma}t}) \frac{\Delta \tilde{\sigma}_r}{\tilde{\sigma}} \rangle. \quad (1)$$

This cross-section increases to $\Delta \tilde{\sigma}_r$ as a result of the absorption events in the layer beyond the initial scattering

$$\Delta \tilde{\sigma}_r t = \left(\frac{\tilde{\sigma}_r}{\tilde{\sigma}}\right) \left(\frac{\tilde{\sigma}_s}{\tilde{\sigma}}\right) \int_{t=0}^t \tilde{\sigma}' dt' e^{-\tilde{\sigma}t'} \int_{\mu} d\mu f(\mu) [1 - P(t', \mu)]. \quad (2)$$

Here: $f(\mu)$ is the angular distribution of the scattered neutrons, assuming that the isotropic scattering $f(\mu) = \text{const}$; $P(t', \mu)$ is the probability of neutron emission after the initial scattering.

Introducing $\mu = 1/\xi$ we can rewrite expression (2) as follows:

$$\begin{aligned} \Delta \tilde{\sigma}_r t &= \frac{1}{2} \left(\frac{\tilde{\sigma}_r}{\tilde{\sigma}}\right) \left(\frac{\tilde{\sigma}_s}{\tilde{\sigma}}\right) \int_{t=0}^t \tilde{\sigma}' dt' e^{-\tilde{\sigma}t'} \left[\int_0^1 d\mu (1 - e^{-\frac{\tilde{\sigma}t'}{\mu}}) + \int_0^1 d\mu' (1 - e^{-\frac{\tilde{\sigma}(t-t')}{\mu'}}) \right] = \\ &= \frac{1}{2} \left(\frac{\tilde{\sigma}_r}{\tilde{\sigma}}\right) \left(\frac{\tilde{\sigma}_s}{\tilde{\sigma}}\right) \int_{t=0}^t \tilde{\sigma}' dt' e^{-\tilde{\sigma}t'} \left[2 - \int_{\xi}^{\infty} \frac{d\xi}{\xi^2} e^{-\tilde{\sigma}t'\xi} - \int_{\xi}^{\infty} \frac{d\xi}{\xi^2} e^{-\tilde{\sigma}(t-t')\xi} \right]. \end{aligned} \quad (3)$$

Expression (3) has to be integrated with respect to E and E' , i.e. an averaging of the type $\langle \rangle = \int dE$ and $\langle \rangle' = \int dE'$ (with respect to the incident neutrons spectrum and the scattered neutron spectrum respectively). This is equivalent to integrating with respect to the total cross-section distributions $\langle \rangle = \int P(\sigma) d\sigma$ and $\langle \rangle' = \int P(\sigma') D\sigma'$. The cross-section distribution functions are obtained from independent calculations of the neutron cross-sections. In the unresolved resonance region they were calculated by the Monte Carlo method based on the R-matrix theory.

Based on a rigorous approach we calculated the corrections for multiple neutron scattering in the sample for typical conditions of measuring the radiative capture cross-section for ^{238}U [3]. The results were compared with those of typical approximation calculations in which the effect of multiple scattering in the constant cross-section approximation was

calculated together with the additional correction for the effect of resonance self-shielding. This method (attributed to Maklin-Smith) is generally used by experimenters to process the results of σ_γ measurements [4-8]. Correction calculations using this method have been carried out by L.E. Kazakov. A comparison is shown in Fig. 2. It can be seen that the approximation method lowers the resulting correction, particularly in the region of low energies, where the effect of the resonance structure is very large. Integrating over the spectrum of a fast reactor core yields a discrepancy of 3-4%.

It is well known that the experimental integral data for the ^{238}U capture cross-section for is systematically 3-4% lower than the corresponding calculated data based on microscopic cross-sections (see for example Ref. [9]). If we assume that there is a systematic error in the microscopic evaluations for ^{238}U associated with the fact that the correction calculated above is too low, as shown in Fig. 2, the contradiction between the microscopic and integral data practically disappears.

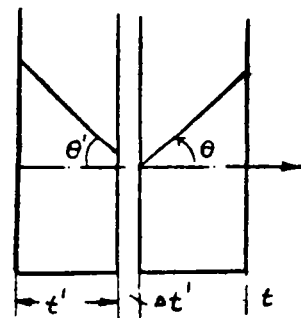


Fig. 1. Geometry used in the calculation of neutron capture after scattering in a layer of thickness t (nucl/b).

The conclusion that the existing method of calculating corrections for finite sample thicknesses in experiments designed to measure the neutron radiative capture cross-section using the gamma-ray recording method is inadequate and applies not only to the experimental data for ^{238}U in the unresolved resonance region, but also to data for other heavy nuclei in both the resolved and unresolved resonance region. The contradictions between the "alpha" measurement results for ^{235}U and ^{239}Pu using different methods are discussed in the literature. Since samples of different thicknesses and dimensions (determined by the transmission, the resolution and other conditions) can be used in various experiment methods, it can be assumed that at least one of the reasons for discrepancies is associated with errors in the

corrections for multiple scattering of resonance neutrons in the detecting equipment.

The most universal method of calculating different equipment corrections is the Monte Carlo method. This method has been increasingly used recently to analyse different kinds of experimental data. In applying this method, it was shown that details of the resonance structure of neutron cross-sections can be represented by so-called subgroup parameters. The extent to which such representations are physically justified, has to be checked in each specific case. As the test calculations for ^{238}U [10] have shown, the subgroup method in the Monte Carlo calculation has yielded results close to those obtained in our calculation.

Using the analytical method in Ref. [10], similar corrections were calculated for the self-indication function

$$T_f(t) = \frac{1}{\sigma_f} \int_0^t \sigma_f(E) \exp[-\sigma_f E] \cdot$$

This type of measurement is described, for example, in Ref. [11] where this correction was disregarded. Figure 3 shows the results of calculating it using the analytical method for conditions in Ref. [11]. It can be seen that the correction is systematic: it grows monotonically as the thickness of the sample increases and with the incident neutron energy decreases.

Since in evaluating the average resonance parameters the experimental data are analysed not only with respect to the average cross-sections but also with respect to the self-indication functions, the latter may also make a contribution to the systematic error in the results of the optimization analysis when evaluating the average resonance parameters. Therefore, evaluations of "pure" average resonance parameters obtained exclusively from the analysis of the resolved resonances, are more reliable. The calculated data of the energy dependence of the average absorption cross-section for ^{238}U in the unresolved resonance region using "pure" average resonance

parameters are in fact lower than the experimental values at low energies in the unresolved regions [12].

From Fig. 2 it follows that if the correction for multiple scattering in the sample is correctly taken into account, there should be a further reduction in the average absorption cross-sections for ^{238}U of approximately 5-6% for the energy group 4.65-10 keV and of 3% for higher energies. Such a correction is similar to fitting evaluated microscopic data by taking integral experiments into account. Consequently, the suggested additional correction, which has a physical explanation, is close to the so-called ABBN-MIKRO and ABBN-78 evaluation [13] (the latter is the result of fitting to the integral data), and eliminates the contradiction between the integral and microscopic experiments.

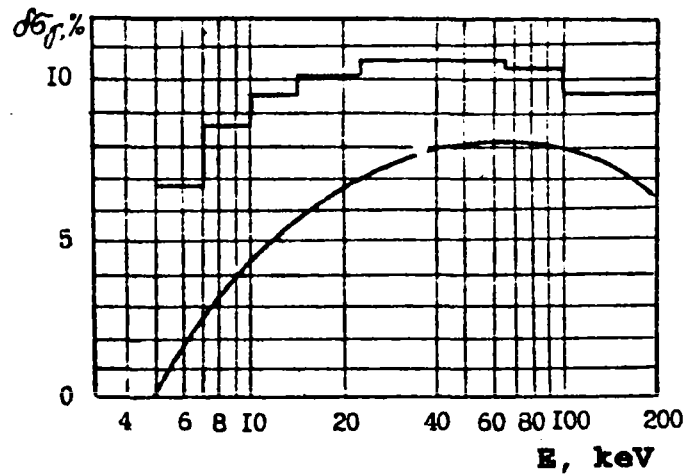


Fig. 2. Resulting correction for a finite thickness ^{238}U sample, $t = 0.00647$ nuc/b.
 -Maklin-Smith method: —
 -Detailed calculation, —

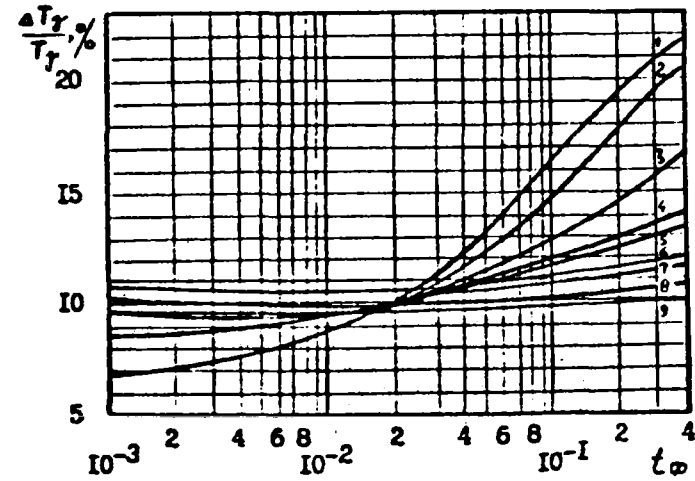


Fig. 3. Resulting correction $\frac{\Delta T_f}{T_f} = \frac{(T_{f,obs} - T_f)}{T_f}$ for finite thickness of metallic ^{238}U sample ($t=0.00647$) as a function of filter thickness T_f for various neutron energy averaged intervals (keV): (1) 4.65-6.78; (2) 6.78-10; (3) 10-14.5; (4) 14.5-21.5; (5) 21.5-31.65; (6) 31.65-46.5; (7) 46.5-67.8; (8) 67.8-100; (9) 100-145.

REFERENCES

- [1] VAN'KOV, A.A., UKRAINTSEV, V.F., et al., Nucl. Sci. Eng. 96 (1987) 122-136.
- [2] VAN'KOV, A.A., TOCHKOV, S.A., UKRAINTSEV, V.F., et al., Method of analysing transmission functions and neutron cross-sections in the unresolved resonance region of heavy nuclides, OIYaI Report 3-84-848, Dubna (1984) [in Russian].
- [3] VAN'KOV, A.A., Calculation of the effects of resonance self-shielding and neutron scattering in a sample in measurements of microscopic neutron radiative capture cross-section: Preprint FEhI-1797, Obninsk (1986) [in Russian].
- [4] KONONOV, V.N., POLETAEV, E.D., BOKHOVKO, M.V., et al., Neutron Physics, M 2 (1980) 280 [in Russian].
- [5] SHORIN, V.C., Correction for multiple neutron scattering in "thin" samples: Preprint FEhI-288, Obninsk (1971) [in Russian].
- [6] SHORIN, V.C., Calculation of resonance self-shielding in measurements of neutron radiative capture cross-sections: Preprint FEhI-342, Obninsk (1972) [in Russian].
- [7] MACKLIN, R.L., Nucl. Instr. Methods 26 (1964) 213-218.
- [8] DRESNER, R., Nucl. Instr. Methods, 16 (1962) 176-188.
- [9] DESAUSSURE, G., SMITH, A.B., ²³⁸U issue, resolved and unresolved, Intern. Conf. on Nuclear Data for Science and Technology, Antwerp (1983) 9-20.
- [10] ANDROSENKO, A.A., ANDROSENKO, P.A., VAN'KOV, A.A., et al., Effective multiple scattering and self-shielding of resonance neutrons in measurements of the average microscopic capture cross-section for ²³⁶U, ²³⁸U and ¹⁹⁷Pu: Preprint FEhI-1849, Obninsk (1987) [in Russian].
- [11] KONONOV, V.N., POLETAEV, E.D., BOKHOVKO, M.B., et al., Neutron Physics, Moscow, 2 (1980) 276 [in Russian].
- [12] VAN'KOV, A.A., UKRAINTSEV, V.F., Questions of atomic science and technology, Ser. nuclear constants, 4 (1987) 58 [in Russian].
- [13] ABAGYAN, L.P., BAZAZYANTS, N.O., NIKOLAEV, M.N., TSIBULYA, A.M., "Group constants for reactor and shielding calculations" ,Moscow, Ehnergoatomizdat (1981) [in Russian].

**THE EFFECT OF $\bar{\nu}(E)$ ENERGY DEPENDENCE AT $E < 1$ eV ON THE
GROUP CONSTANTS OF ^{239}Pu IN THE LOWER ENERGY GROUPS**

A.G. Gusejnov, M.A. Gusejnov, N.S. Rabotnov

ABSTRACT

The effect of the energy dependence of the average number of prompt neutrons on the ^{239}Pu fission BNAB-26 group cross-sections has been estimated. It was also found that the values of $\bar{\nu}(E)$ are lowered by approximately 1% when the temperature increases from 300 °K to 2000 °K. Taking this dependence into account may improve the predictability of the plutonium-fueled reactor characteristics.

Measurement of the average prompt fission neutrons $\bar{\nu}(E_n)$ in the reaction $^{239}\text{Pu}(n,f)$ at $E_n \leq 1$ eV indicate that there is noticeable energy dependence of $\bar{\nu}(E_n)$ in this region [1-4]. The authors of Ref. [5] performed precision measurements of the average kinetic energy of fission fragments emitted in the same reaction for the same energy region. By comparing these results with the systematics data in Refs. [1-4] using energy balance, they concluded that the physical cause of the variations in $\bar{\nu}(E_n)$ and $\bar{E}_k(E_n)$ was a difference of the order of 2% in the values of $\bar{\nu}$ for the 0^+ and 1^+ states of the compound nucleus corresponding to the binding energy of the "negative" (0^+) ^{240}Pu level and to the first resonance at $E_n^0 = 0.299$ eV(1^+). The figure shows a system of the type used in Ref. [5]. The same symbols are used for points taken from various sources. Detailed references may be found in Ref. [5]. We evaluate the influence of this effect on the mean value $\bar{\nu}$ used in the 26-group set [6] for low energy groups, in particular, we evaluate the effect it has on their

dependence on the neutron spectrum temperature and dilution cross-section taking resonance self-shielding into account. (From this point on, for the sake of brevity, E will be used to signify E_n).

The experimental data points in the figure shows the average number of prompt neutrons per fission at given incident neutron energies. Assuming that the $\bar{\nu}(E)$ values are different for the two spin subsystems but are not in themselves energy dependent, the $\bar{\nu}(E)$ dependence can be expressed by

$$\bar{\nu}(E) = \left[\sigma_f^1(E) \bar{\nu}^1 + \sigma_f^0(E) \bar{\nu}^0 \right] / \left[\sigma_f^1(E) + \sigma_f^0(E) \right], \quad (1)$$

where $\bar{\nu}^0$ and $\bar{\nu}^1$ are the values of $\bar{\nu}$ for the 0^+ and 1^+ resonances, and $\sigma_f^i(E)$ are the contributions of the individual resonances to the fission cross-section.

The continuous thick line in the figure represents the dependence calculated using expression (1) as given in Ref. [5]. We calculated this curve in a two-resonance approximation, i.e. assuming that only the two above-mentioned resonances contribute to the total and fission cross-sections (in fact, in the energy region in question, their contribution accounts for approximately 90% thereof). The two curves are very close to one another. In this calculation we used the resonance parameters for ^{239}Pu given in Ref. [7]. The cross-sections, which are measured in barns, take the following form (ignoring the Doppler effect):

$$\sigma_t(E) = 0,6537/\sqrt{E} \sum_{j=0,1} \frac{G_j^t + H_j^t [(E - E_j^0)/\delta_j]}{\delta_j \left\{ 1 + [(E - E_j^0)/\delta_j]^2 \right\}} + \sigma_{\text{pot}}; \quad (2)$$

$$\sigma_f(E) = 0,6537/\sqrt{E} \sum_{j=0,1} \frac{G_j^f + H_j^f [(E - E_j^0)/\delta_j]}{\delta_j \left\{ 1 + [(E - E_j^0)/\delta_j]^2 \right\}}. \quad (3)$$

The numerical values for the parameters are given in Table 1 for $\sigma_{\text{tot}} = 10.2$ b.

For the \bar{v}^j coefficients in expression (1) we used values of $\bar{v}^0 = 2.886$ and $\bar{v}^1 = 2.827$ normalized to the value of $\bar{v} = 2.862$ for thermal neutrons (this corresponds to the curve from Ref. [5] and using $\Delta v = \bar{v}^0 - \bar{v}^1 = 0.059$, also taken from Ref. [5]).

First, let us evaluate the simplest effect - namely the dependence of \bar{v} , averaged over the Maxwellian neutron spectrum on the temperature of that spectrum

$$\langle \bar{v} \rangle (T) = \frac{\int_0^{\infty} dE \phi(E, T) [\bar{v}^0 \sigma_f^0(E) + \bar{v}^1 \sigma_f^1(E)]}{\int_0^{\infty} dE \phi(E, T) [\sigma_f^0(E) + \sigma_f^1(E)]}, \quad (4)$$

where $\phi(E, T) = 2\sqrt{E} \exp(-E/kT) / \sqrt{\pi(kT)^3}$.

The values obtained for $T = 300-10000$ are also represented in the figure (by large dots); the temperature T is expressed in eV. The $\langle \bar{v} \rangle (T)$ dependence does not repeat $\bar{v}(E)$, but the maximum extent of the effect (reduction in $\langle \bar{v} \rangle$) amounts to approximately 1%.

Various cross-section attributes for the twenty-fifth and twenty-fourth groups of the 26 group set were also calculated in order to illustrate the influence of the $\bar{v}(E)$ energy dependence on the mean values of $\langle \bar{v} \rangle (T)$ which may be obtained by taking the resonance self-shielding of the cross-sections into account. The following group averages were calculated: $\langle 1/(\sigma_t + \sigma_0) \rangle_{\Delta E}$; $\langle \sigma_t / (\sigma_t + \sigma_0) \rangle_{\Delta E}$; $\langle v \sigma_t / (\sigma_t + \sigma_0) \rangle$, where ΔE is the energy interval over which averaging is performed, σ_0 is the dilution cross-section, for $\Delta E_{25} = 0.215-0.465$ eV and $\Delta E_{24} = 0.465-1$ eV, $\sigma_0 = 0$ and $\sigma_0 = 100$ b respectively. As above, $\langle \rangle$ indicates averaging over the Maxwellian spectrum, and $v \sigma_t$ is an abbreviation for $(\bar{v}^0 \sigma_f^0 + \bar{v}^1 \sigma_f^1)$. The symbol $\langle 1 \rangle$ stands for normalization - the spectrum

integral over the ΔE interval. The results are given in Table 2 which also gives some relations for these attributes including the integrated value of the self-shielded value of $\bar{\nu}$:

$$\langle \bar{\nu} \rangle (T, \sigma_0) = \langle \nu \sigma_f / (\sigma_t + \sigma_0) \rangle / \langle \sigma_f / (\sigma_t + \sigma_0) \rangle . \quad (5)$$

Clearly, the self-shielded $\langle \bar{\nu} \rangle$ value for the twenty-fifth group is hardly dependent on the neutron spectrum temperature. As for the twenty-fourth group, it is only slightly dependent, and in contrast to the not self-shielded value, averaged over the total spectrum, it increases with T. However, both values, at $kT = 0.0253$ eV for instance, are significantly lower than the "thermal" $\bar{\nu}$ value for monoenergetic neutrons at $E = 0.0253$ eV.

Because of the approximations used, the evaluated values presented in this paper are not precise; they do suggest, however, that if a more precise method were to be used to estimate the $\bar{\nu}(E)$ dependence effect, it could help improve the liability of the characteristics of thermal systems using plutonium fuel.

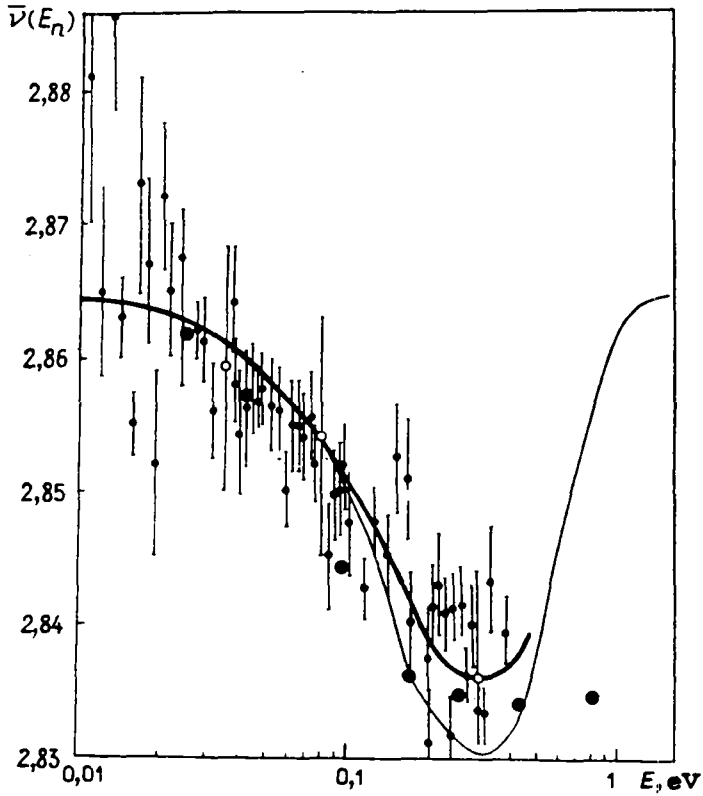


Figure. Dependence of the average number of prompt neutrons for ^{239}Pu at a fission induced neutron energy of < 1 eV:
 • - experimental data systematized in Ref. [1],
 ● - results obtained by averaging over the Maxwellian spectrum [4];
 ○ - conversion into $\bar{\nu}(E_n)$ of the dependence on E_n of the mean kinetic energy of the fragments as measured in Ref. [1];
 - the continuous lines are the calculated $\bar{\nu}(E_n)$ dependences assuming that the values differ by 0.059 for the $0+$ and $1+$ resonances;
 - the thick line is taken from Ref. [1],
 - the thin line was calculated by us in a two-resonance approximation whose

Table 1

Resonance parameters for the ^{239}Pu cross-section structure to obtain cross-sections in barns using expressions (2) and (3) for energies smaller than 1 eV [7]

E_J^0, eV	J	G_J^f	H_J^f	G_J^t	H_J^t	δ_J
-0,260	0	0	31,92	0	45,21	0,100
0,299	1	129,08	3,32	220,76	3,07	0,0471

Table 2

Dependence of cross-section parameters averaged over the 24th and 25th groups on a Maxwellian spectrum temperature T.

T, K (eV)	Functionals				
	$\langle 1/(\sigma_t + \sigma_0) \rangle$	$\langle \sigma_f/(\sigma_t + \sigma_0) \rangle$	$\langle \nu \sigma_f/(\sigma_t + \sigma_0) \rangle$	$\langle \frac{\nu \sigma_f}{\sigma_t + \sigma_0} \rangle / \langle \frac{1}{\sigma_t + \sigma_0} \rangle$	$\langle \frac{\nu \sigma_f}{\sigma_t + \sigma_0} \rangle / \langle \frac{\sigma_f}{\sigma_t + \sigma_0} \rangle$
For the 24th group $\Delta E = (0.465 - 1.0)$ eV, $\sigma_0 = 0$ barns					
300(0,0253)	2,951(-3)	5,832(-1)	1,656	561,3	2,340
500(0,04217)	3,413(-3)	5,825(-1)	1,654	479,2	2,840
1000(0,08433)	4,730(-3)	5,790(-1)	1,646	343,7	2,644
2000(0,16867)	5,902(-3)	5,720(-1)	1,628	235,9	2,646
3000(0,2530)	3,359(-3)	5,679(-1)	1,617	200,7	2,643
5000(0,4217)	3,142(-3)	5,539(-1)	1,607	175,8	2,650
10000(0,8433)	1,001(-4)	5,303(-1)	1,593	159,6	2,851
For the 24th group $\sigma_0 = 100$ barns					
300(0,0253)	2,253(-3)	4,515(-1)	1,282	537,9	2,840
500(0,04217)	2,509(-3)	4,335(-1)	1,239	493,9	2,840
1000(0,08433)	3,032(-3)	4,011(-1)	1,143	372,3	2,643
2000(0,16867)	3,733(-3)	3,573(-1)	1,017	266,7	2,615
3000(0,2530)	4,133(-3)	3,553(-1)	9,543(-1)	230,9	2,647
5000(0,4217)	4,445(-3)	3,156(-1)	8,939(-1)	202,3	2,643
10000(0,8433)	4,534(-3)	3,004(-1)	8,559(-1)	182,7	2,649
For the 25th group $\Delta E = (0.215 - 0.465)$ eV, $\sigma_0 = 100$ barns					
300(0,0253)	4,114(-4)	5,652(-1)	1,600	3889	2,831
500(0,04217)	3,735(-4)	5,531(-1)	1,602	4222	2,830
1000(0,08433)	4,272(-4)	5,621(-1)	1,590	3724	2,830
2000(0,16867)	5,233(-4)	5,539(-1)	1,573	3008	2,830
3000(0,2530)	5,631(-4)	5,530(-1)	1,585	2750	2,830
5000(0,4217)	5,07(-4)	5,504(-1)	1,558	2551	2,831
10000(0,8433)	3,442(-4)	5,433(-1)	1,552	2409	2,831

REFERENCES

- [1] BOLDEMAN, J.W., Proc. Intern. Specialists Symp. on Neutron Standards and Applications, Gaitersburg: NBS SP 493 (1977) 182.
- [2] WEINSTEIN, REED, R., BLOCK, R.C., Proc. 2nd IAEA Symp. on Physics and Chemistry of Fission, Vienna (1969) 447.
- [3] HOCKENBURY, R.W., REED, R.L., BLOCK, R.C., Proc. 3rd IAEA Symp. on Physics and Chemistry of Fission, Vol. 2, Rochester (1973) 502.
- [4] GWIN, R.L., SPENCER, R.R., INGLE, R.W., Nucl. Phys. Sci. and Engng. 87 (1984) 381.
- [5] WALSH, R.L., BOLDEMAN, J.W., Nucl. Phys. A451 (1986) 113.
- [6] ABAGYAN, L.P., et al., Group constants for reactor calculations and protection, Ehnergoizadat, Moscow (1981) [in Russian].
- [7] KOLESOV, V.V., LUK'YANOV, A.A., Preprint FEhI-1404-2, Obninsk (1983) [in Russian].

Submitted for publication 25 January 1988

**TESTING OF THE ^{235}U , ^{238}U AND ^{239}Pu CROSS-SECTION
RESONANCE STRUCTURE DATA IN THE UNRESOLVED RESONANCE
REGION USING TRANSMISSION EXPERIMENTS**

V.N. Koshcheev, E.V. Dolgov and A.M. Tsibulya

ABSTRACT

Subgroup parameters of ^{235}U , ^{238}U and ^{239}Pu in the unresolved resonance region used in the MULTIK multigroup data system have been tested using transmission experiments. Calculated and experimental data were found to be in agreement. The need for experimental transmission data as well as information on the resolved resonance region for the evaluation of the cross-section resonance structure in the unresolved region is emphasized.

Information on the cross-section resonance structure in the unresolved resonance region occupies a special place among the various types of neutron-nuclide interaction characteristics. This is because the cross-section structure is described in terms of average resonance parameters, evaluated using the results of indirect experiments and theoretical models of the cross-section structure. It is clear that the reliability of the data thus obtained increases as the range of heterogeneous experiments on which they are tested is widened.

Evaluated neutron data files, particularly the FOND library [1], include average resonance parameters which have been obtained, first by averaging resonance parameters from the

unresolved resonance region and, then by correcting them in such a way as to produce a correct description of the energy dependence of the observed neutron cross-sections, averaged over many resonances, in the unresolved region. In Ref. [2], subgroup parameters were obtained using the contribution of temperature independent subgroup based on a set of this type of data for ^{235}U , ^{238}U and ^{239}Pu . It is rather difficult to assess the accuracy of the resonance self-shielding effects calculated using these parameters since evaluations of this type are carried out in the framework of a concrete theoretical model to describe cross-sections. For example, for ^{238}U various authors give close and rather high evaluations of the accuracy values of the cross-section self-shielding contribution [3-5], on the other hand, the discrepancies between the evaluations often exceed the expected uncertainty range. For ^{235}U and ^{239}Pu , theoretical modelling of the cross-section structure is less reliable because of the presence of the fission channel and the high density of the resonance levels, with the result that the reliability of existing resonance structure evaluations is even lower. In the light of this, it is extremely important to test the evaluated resonance structure of the cross-section in the unresolved resonance region against an independent group of experimental data. This is the aim of the present paper.

We present results of tests of ^{235}U , ^{238}U and ^{239}Pu subgroup parameters in neutron transmission experiments for various sample thicknesses of the investigated materials. These subgroup parameters [2] are currently used in the MULTIK multigroup sets of data [6]. The idea of using neutron flux transmission curve measurements right up to extreme attenuation as an information source for cross-section structure in the unresolved resonance region was proposed by M.N. Nikolaev and first carried out in Ref. [7]. Recently interest in this method has grown sharply, but as yet the amount of information accumulated is not very great.

COMPARED VALUES

Experiment

The following transmission results have been obtained in the neutron transmission experiments for the nuclides under investigation:

$$\text{Total transmission: } \tau_t^{\text{exp}}(n) = \int \varphi(E) \exp(-n\sigma_t) dE / \int \varphi(E) dE$$

$$\text{Partial transmission: } \tau_x^{\text{exp}}(n) = \int \varphi(E) \sigma_x(E) \exp[-n\sigma_t(E)] dE / \int \varphi(E) \sigma_x(E) dE$$

where $\varphi(E)$ is the neutron flux spectrum, n is the thickness of the sample under investigation, and $\sigma_t(E)$ and $\sigma_x(E)$ are the total and partial interaction cross-sections, respectively.

Occasionally, as a result of the processing of the experimental data, the following effective cross-sections were obtained:

$$\sigma_{tt}^{\text{exp}}(n) = -\frac{1}{n} \ln[\tau_t^{\text{exp}}(n)]; \quad \sigma_{tx}^{\text{exp}}(n) = -\frac{1}{n} \ln[\tau_x^{\text{exp}}(n)].$$

It is easy to see that

$$\lim_{n \rightarrow 0} \sigma_{tx}^{\text{exp}}(n) = \int \varphi(E) \sigma_x(E) \sigma_t(E) dE / \int \varphi(E) \sigma_x(E) dE = \langle \sigma_t \sigma_x \rangle / \langle \sigma_x \rangle ;$$

$$\lim_{n \rightarrow 0} \sigma_{tt}^{\text{exp}}(n) = \int \varphi(E) \sigma_t(E) dE / \int \varphi(E) dE = \langle \sigma_t \rangle ,$$

where $\langle \rangle$ denotes averaging over the energy interval. The last value is a total cross-section averaged over the resonance characteristics having the weight of a partial cross-section.

To obtain boundary values it would have been particularly important to have reliable data for thin samples of the investigated nuclide. However, these were the least accurate data obtained in the experiment.

As a rule, the Fermi spectrum $\varphi(E)$ was used as the averaging spectrum in the averaging interval.

Calculation

In the ABBN-78 [3] and MULTIK [6] group data, which were used in the calculations, the Fermi spectrum $\varphi(E)$ was used as the averaging spectrum in the investigated region.

Using subgroup parameters it is possible to express the total transmissions in the form of

$$\tau_t^{cal}(n) = \sum_i a_i \exp(-n\sigma_{t,i}),$$

and partial transmissions by

$$\tau_x^{cal}(n) = \sum_i a_i \sigma_{x,i} \exp(-n\sigma_{t,i}) / \sum_i a_i \sigma_{x,i},$$

where a_i is the fraction of subgroup i , $\sigma_{t,i}$ and $\sigma_{x,i}$ are the subgroup total and partial interaction cross-sections, respectively. It is easy to obtain the effective cross-sections by analogy using the experimental data:

$$\sigma_{tt}^{cal}(n) = -\frac{1}{n} \ln[\tau_t^{cal}(n)]; \quad \sigma_{tx}^{cal}(n) = -\frac{1}{n} \ln[\tau_x^{cal}(n)].$$

In the calculations we used the normalized subgroup parameters, a_i , k_{ti} , k_{si} , k_{ci} , k_{fi} taken from Ref. [2]. The subgroup cross-sections were determined by

$$\sigma_{ti} = \sigma_t k_{ti}; \quad \sigma_{ei} = \sigma_e k_{ei}; \quad \sigma_{ci} = \sigma_c k_{ci}; \quad \sigma_{fi} = \sigma_f k_{fi}.$$

Here σ_t , σ_e , σ_c and σ_f are the total, scattering, capture and fission multigroup cross-sections, respectively (taken from the MULTIK multigroup sets of data), derived from files of evaluated neutron data given in the FOND data library [1] and using the GRUKON software package [8], all data but σ_t for ^{238}U , were taken from Ref. [9]. In addition, calculations were made using the subgroup parameters of the ABBN-78 group data, as well as with the evaluated parameters [10,11]. All the calculated values were averaged over the energy intervals in accordance with the MULTIK or ABBN group data nomenclature, respectively.

Testing of the ^{238}U data

Several transmission experiments have already been carried out to measure the basic ^{238}U resonance absorber: four of them using the radiative capture self-indication technique. The experimental data measured in these experiments which were used to test the calculated data are listed in the following Table.

LIST OF ^{238}U TRANSMISSION EXPERIMENTS

Refs	Listed quantity	Energy region (keV)	Number of thicknesses	atoms per barn
12	T_t	0.46 - 120	11	0.0047- 1.060
13	T_t	4.65 - 200	10	0.0142-0.615
14	T_t, T_c	10 - 80	5	0.005-0.0943
15	T_t, T_c	5 - 110	7	0.047-0.190
16	T_e	1 - 100	8	0.0024-0.305
17	σ_{tt}	55 and 144	7	0.0094-0.279
18	T_t	10.2 - 91.9	5	0.0076-0.0621
19	σ_{tt}, σ_{tc}	1.0 - 10.2	5	0.0076-0.0621
20	σ_{tt}	66 and 205	6	0.006-0.092
21	T_t	24 and 144	15	0.010-0.266
22	σ_{tt}	24.3 - 649.1	4	0.0063-0.0807
23	σ_{tt}	3.04 - 4.0	4	0.0237-0.140
24	σ_{tt}	24 and 144	8	0.023-0.240
25	T_c	4.0 - 10.0	4	0.0038-0.0521
26	T_c	4.0 - 5.0	11	0.0074-0.144

from Fig. 4, it is impossible to determine this law with sufficient accuracy on the basis of experimental data alone as the data spread is too great. As a rule, extrapolation is based on a description of the cross-section structure in terms of average resonance parameters. Variation in these parameters can have a considerable influence on the $\sigma_{tt}(n)$ dependence.

It follows from the analysis carried out that a correct evaluation of the average resonance parameters should use the $T_t^{\text{exp}}(n)$ transmissions themselves as initial data and not the total cross-sections σ_t deduced from them. If it were possible to unequivocally describe the available $\sigma_c(E)$, $T_t^{\text{exp}}(n, E)$ and $T_c^{\text{exp}}(n, E)$ data, then agreement between $T_t^{\text{exp}}(n, E)$ and $T_t^{\text{cal}}(n, E)$ for thick samples in the 5-200 keV energy region would be guaranteed because of the increase in the subgroup cross-section $\sigma_{t,i}$ in subgroup i for low values of $\sigma_{t,i}$ and $\sigma_{c,i}$, which would only arise in $T_t(n, E)$ at large values of n and would have virtually no effect on the value of $T_c(n, E)$. At the present time, evidently, only one paper [15] has done this. The analysis also shows, in our view, that much remains to be done to improve the accuracy of experimental T_t and T_c ^{238}U transmission data.

Testing of the ^{235}U data

There is little experimental information on ^{235}U transmissions: in 1969 data were published on fission transmissions [29], followed by the presentation of revised data of the experiment in 1979 [30] which aimed to reduce the error of the old data. Finally, in 1979 data appeared in Ref. [10] on total and fission transmissions .

Figure 5 shows how MULTIK and BNAB-78 calculations describe experimental effective cross-section $\sigma_{tt}(n)$. The calculations were carried out using ABBN energy group data. From the figure, it can be seen that the existing MULTIK and ABBN-78 data which are quite divergent in several groups, do not on the whole contradict one single experiment [10]. Clearly new experimental

Figure 1 shows the energy dependence of calculated and experimental transmission values $T_t(E)$ for three sample thicknesses. It can be seen from that figure that, on the whole, the multigroup curve describes the experimental data quite well, especially for thin samples. As the thickness of the sample increases, there is a tendency for the calculated and experimental data to diverge in the 50-200 keV energy region. At the same time, as can be seen from Fig. 2, the data obtained by the capture self-indication technique agrees well with the calculated data for all energy regions and thicknesses. By examining the total transmission data $T_t(E,n)$ only, we get the impression that the total cross-section used in the multigroup calculations is a little too high in the 50-200 keV energy region.

At the same time, the experimental data describe the energy dependence of both the total cross-section and the radiative capture cross-section quite well (Fig. 3). However, the experimental cross-sections shown in Fig. 3a are nothing else but the result of an extrapolation of the effective cross-section $\sigma_{tt}(n)$ to zero thickness. How reliable this extrapolation is can be seen from Fig. 4 which shows the dependence of effective cross-sections $\sigma_{tt}(n)$ for the two energy intervals 10.0-21.5 keV (11th ABBN group) and 21.5-46.5 keV (10th BNAB group). In the first, the total cross-section σ_t of the intervals in MULTIK is somewhat lower than experimental data [18], whereas in the second, it is higher (see Fig. 3a). It can be clearly seen from Fig. 4 that in the 11th group the $\sigma_{tt}(n)$, the multigroup parameter curve, lies lower than the data in Ref. [18], not only when $n \rightarrow 0$ but also for finite values of n . In the 10th group, the experimental points from [18] lie lower than the MULTIK calculation, except for the first two points where n is thin and where the statistical error and the probability of undetected systematic errors are high. It is evident that by extrapolating to zero thickness (i.e. the deduced total cross-section σ_t) depends considerably on what law is being used to estimate the dependence of the effective cross-section $\sigma_{tt}(n)$. As can be seen

data are required for a more accurate determination of the discrepancies to be made.

Figure 6 shows the effective cross-section $\sigma_{t,r}$ as a function of the sample thickness under investigation. According to the data shown in the figure, the experimental data points are well described by calculation. The experimental results are in better agreement with the multigroup parameters in groups 15, 14 and 13 than with the ABBN-78 calculations. In groups 17, 16 and 12 both calculations are equally good. Finally, in group 11 the BNAB-78 system describes experimental data perhaps better than MULTIK, although the data spread here considerably exceeds the discrepancy between the two calculations.

On the whole, the transmission data confirm the predictions of the ^{235}U cross-section structure on which the evaluated neutron data in the FOND library are based.

Testing of the ^{239}Pu data

At the present time, two sets of experimental data are known to exist for ^{239}Pu : in 1967, data were published on fission transmissions T_f [31], and in 1979 the results of an experiment on total T_t and fission T_f transmissions appeared [11].

Figure 7 shows how MULTIK, ABBN-78 and subgroup parameter calculations based on Ref. [11] data describe the experimental dependence of the effective cross-section $\sigma_{tt}(n)$. It can be seen that on the whole good agreement is observed between the single experiment and the calculated values, with the exception perhaps of groups 17 and 16. In these groups, calculations were not carried out using the parameters given in Ref. [11] since the sum of the subgroup contributions in these energy groups had not been normalized to unity, and the average cross-sections, deduced from the subgroup parameters, do not coincide with the cross-sections from which the parameters were derived. As regards the description of the resonance structure in groups 17 and 16, a

more correct description is evidently obtained if three subgroups, and not two as was done in MULTIK, are used.

Figure 8 shows a similar comparison of calculated and experimental data for $\sigma_{tf}(n)$. As can be seen from the figure, in this case, a better agreement of calculation with experiment is actually observed in the low-energy groups. As energy increases from groups 15 to 11, experimental values for $\sigma_{tf}(n)$ are shown to be systematically higher than the calculated values for thin samples where $n < 10^{-2}$ atom/b. It is difficult to understand such curve behavior if the cross-section structure is described within the framework of the given model, i.e. in terms of average resonance parameters. Thus, the evaluations carried out quite independently in Refs [32] and [11] for groups 14 to 11 give an almost identical shape of the curve $\sigma_{tf}(n)$. In addition, the curve becomes thickness-independent for thin samples. From this point of view it is curious that $\sigma_{tf}^{cal}(n)$, as calculated by using ABBN-78 subgroup parameters, displays behavior analogous to that observed in experiment. This behavior of the curve is observed because in BNAB-78 the ratio of the fission cross-section of the maximal and minimal subgroups is much larger than assumed in contemporary evaluations, and so the role of the subgroup with a high cross-section is particularly emphasized for thin samples.

It should be remembered that subgroup description of cross-section resonance structure for ^{239}Pu is still the same in ABBN-78 as in BNAB-70 [33]. The subgroup parameters were combined to describe the dependence of the self-shielding cross-section coefficients on the dilution cross-sections which were evaluated already in 1962. Of course, the reliability of the old data is not high and there is no reason to give them preference over contemporary evaluations, as for the indicated energy groups, they are seen to diverge from the only experiment.

In conclusion, it should be noted that on the whole, the experimental ^{235}U , ^{238}U and ^{239}Pu transmission function data support predictions of the cross-section structure of these

nuclei in the unresolved resonance region, which were based on extrapolation of cross-section structure characteristics from the resolved resonance region and on theoretical description of the energy dependence on average cross-sections in the same unresolved resonance region. For ^{235}U and ^{239}Pu available experimental transmission function data are clearly insufficient; it would be very useful to obtain new information. The present discrepancies for ^{239}Pu are still not sufficiently established to justify making changes in the data used. In the case of ^{238}U , it would seem that the reliability of the average resonance parameters might, , be considerably raised if experimental data on transmissions $T_t(n,E)$ and $T_c(n,E)$ were used in their evaluation instead of total cross-section data. Additional experimental data will be useful if they can compete with available data.

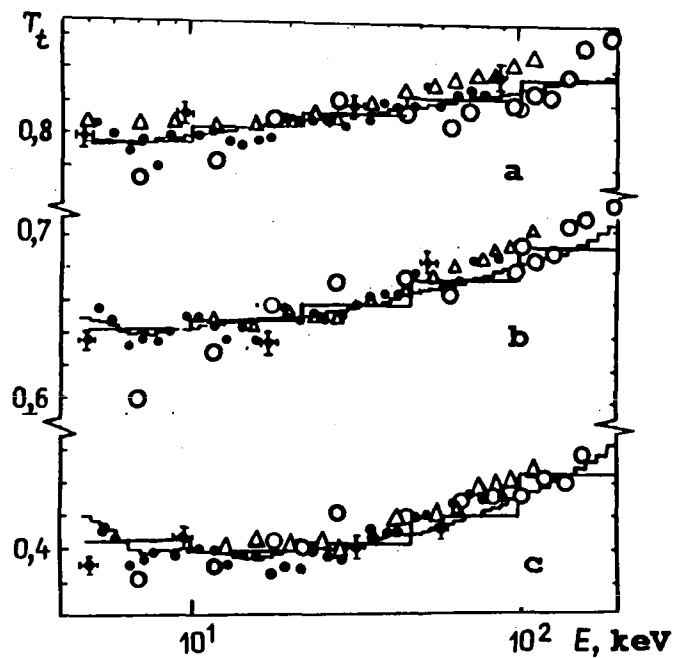


Fig. 1. Energy dependence of total transmissions T_t for various sample thicknesses of ^{238}U , atom/b:

- a) $n = 0.0155$;
- b) $n = 0.0316$;
- c) $n = 0.0707$.

Calculation:

- using MULTIK
- using BNAB-78

Authors' data

- ○ : [13],
- ▲ : [15],
- ● : [18,19].

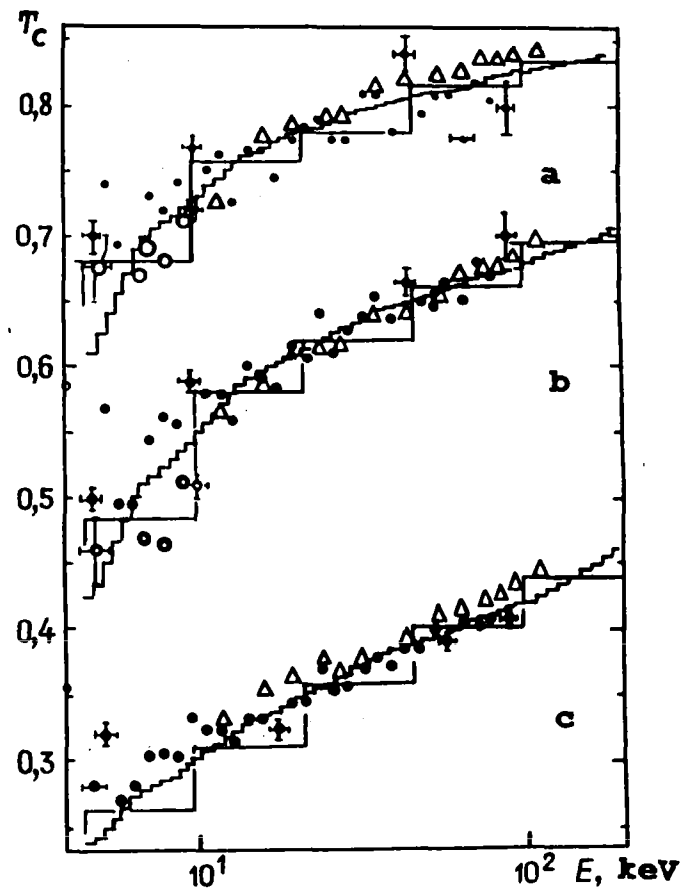


Fig. 2. Energy dependence of capture transmissions T_c for various sample thicknesses of ^{238}U , atom/b:

- a) $n = 0.0155$,
- b) $n = 0.0316$;
- c) $n = 0.0707$.

Calculation:

- using MULTIK
- using BNAB-78.

Authors' data

- : [25],
- ▲ : [15],
- : [18,19].

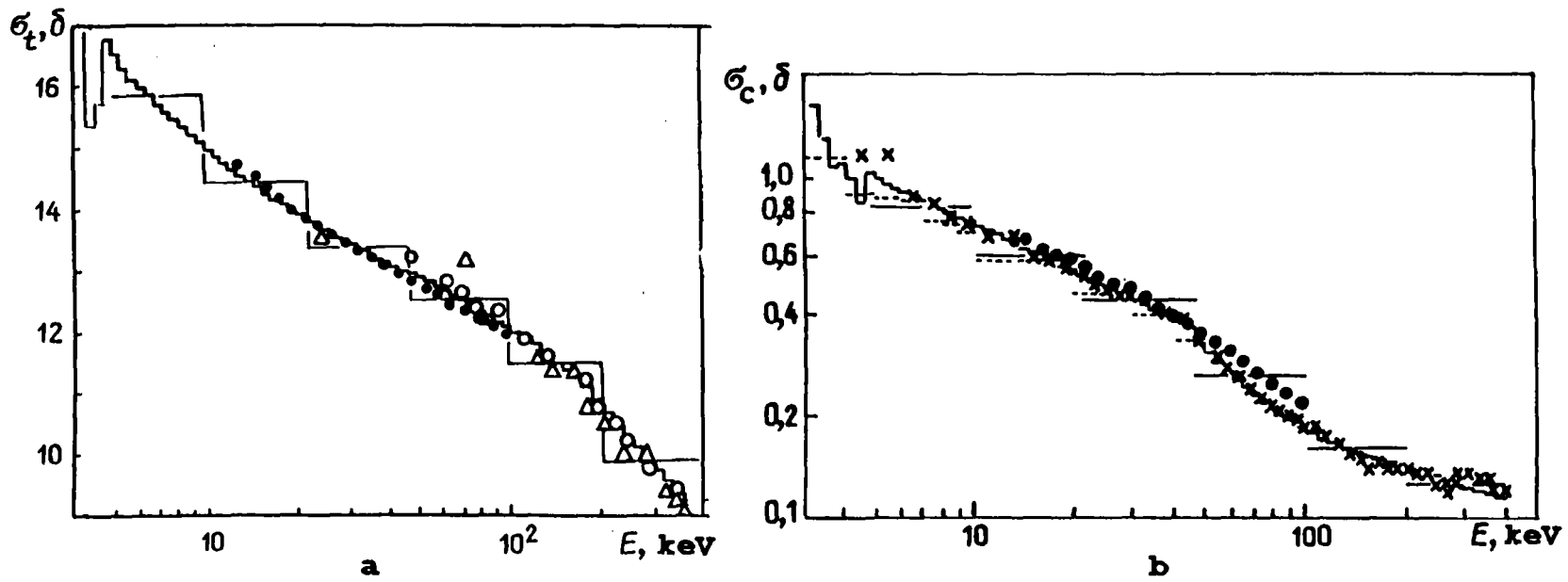


Fig. 3. Energy dependence of the total cross-section (a) and the radiative capture cross-section (b) of ^{238}U .
 Data: MULTIK \sim ; BNAB-78 — ; \circ - [20]; Δ - [22]; \bullet - [19];
 \times - [27]; - - - - [28].

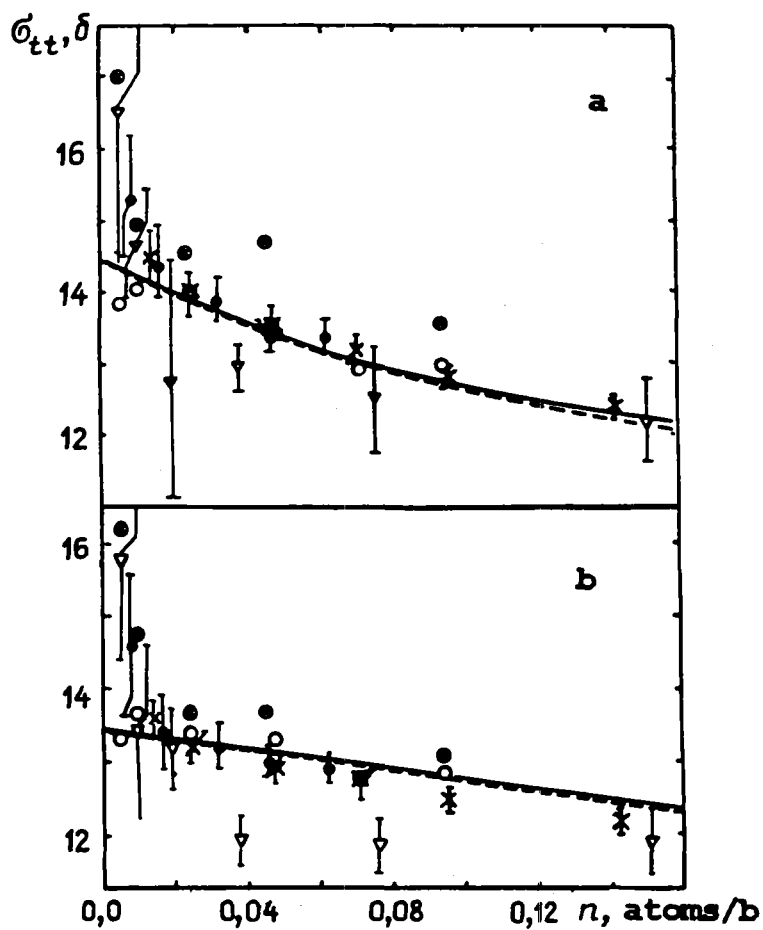


Fig. 4. Comparison of the ^{238}U effective total cross-section $\sigma_{tt}(n)$ for energy groups 11 (a) and 10 (b).

Calculation:

———— using MULTIK;

----- using BNAB-78.

Authors' data: α - [12]; X - [13];

\circ - [14]; \circ - [15]; \bullet - [18].

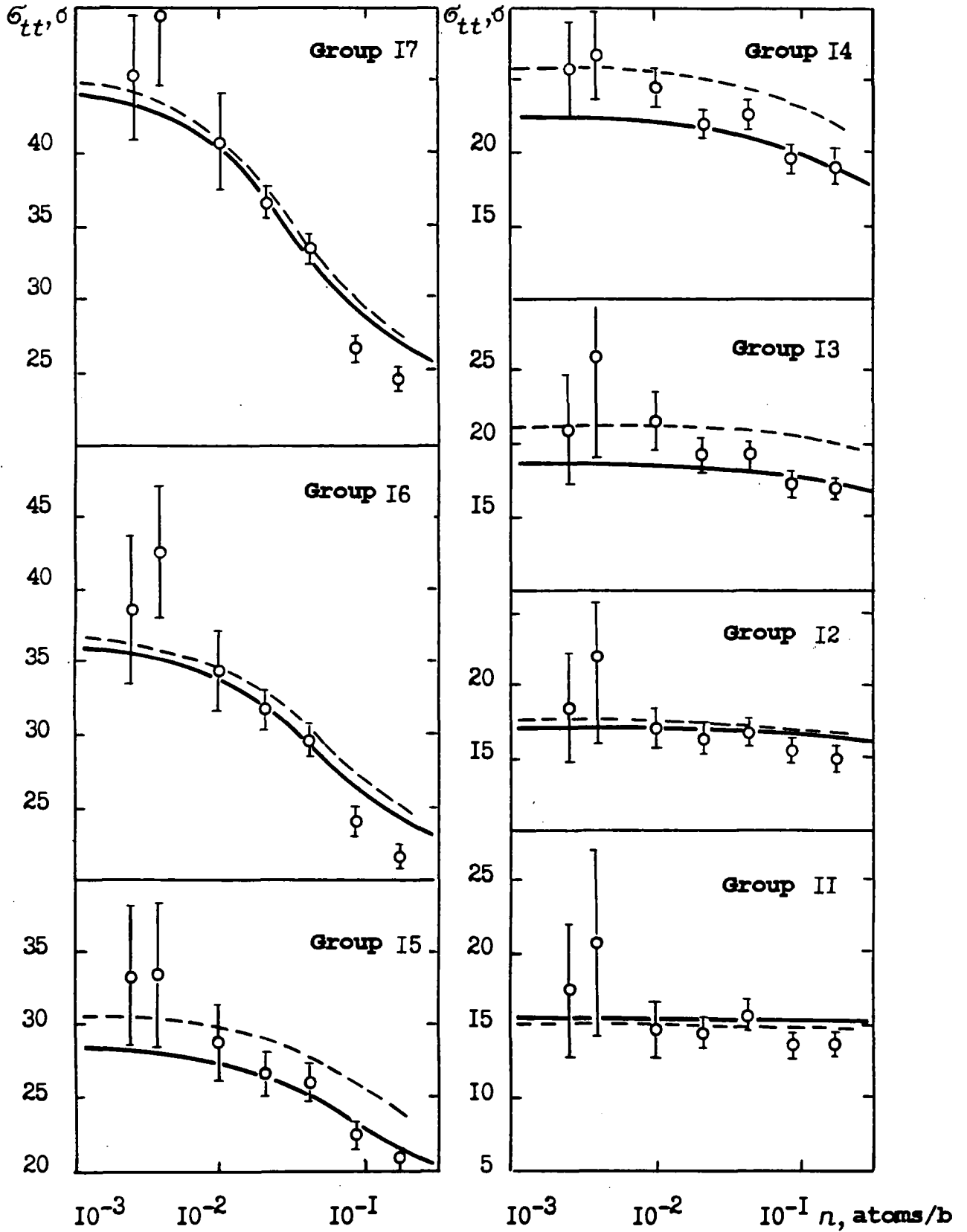


Fig. 5. Comparison of the effective ^{235}U total cross-section $\sigma_{tt}(n)$ within each energy group.
Calculation: — using MULTIK; - - - - using BNAB-78;
o - data from Ref. [10].

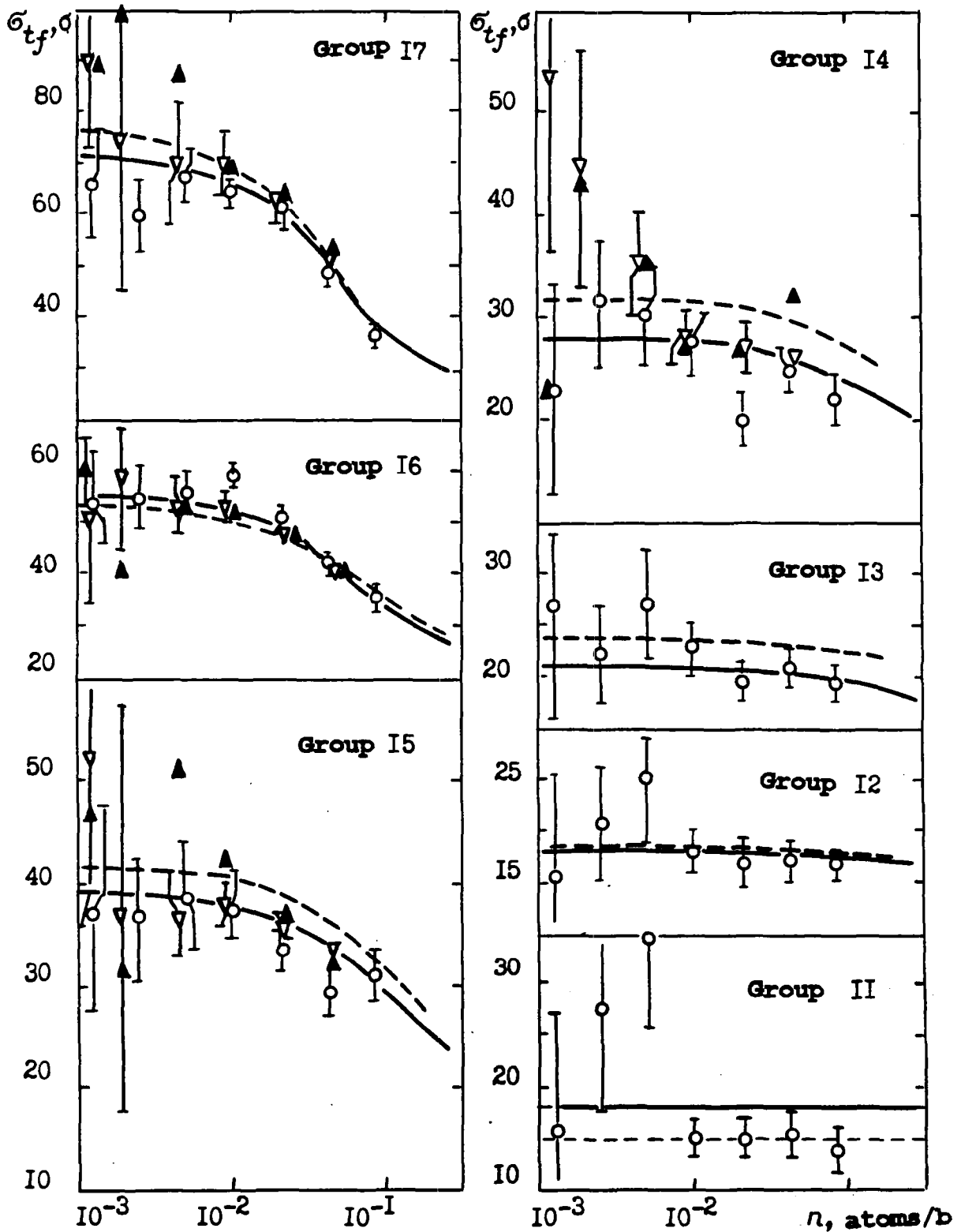


Fig. 6. Comparison of the effective ^{235}U cross-section $\sigma_{t,f}(n)$ within each energy group.

Calculation: ——— using MULTIK; - - - - - using BNAB-78.

Authors' data: 0 - 410]; Δ - [29]; α - [30].

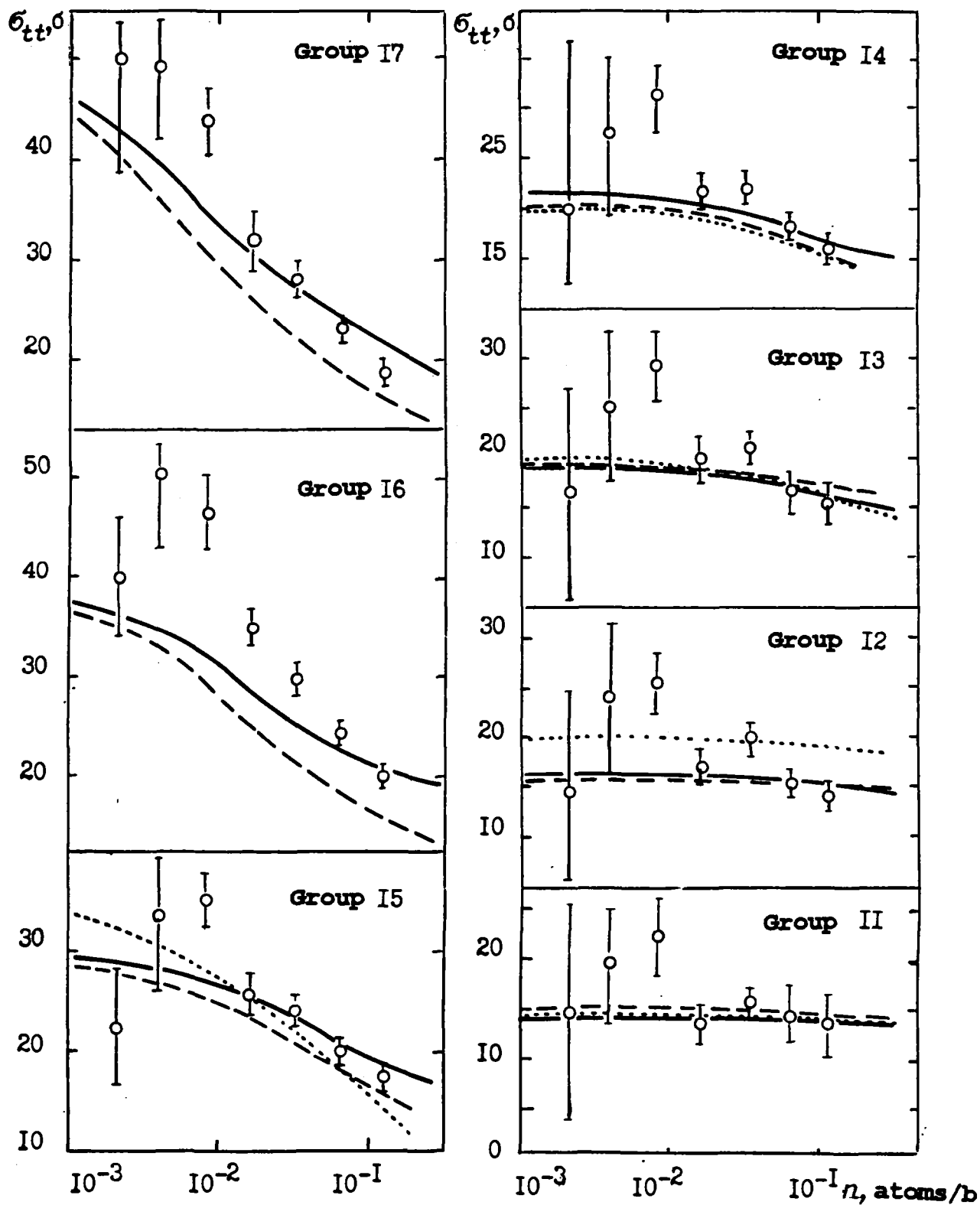


Fig. 7. Comparison of the effective ^{239}Pu cross-section $\sigma_{tt}(n)$ within each energy group. Calculation: — using MULTIK; - - - - using BNAB-78; using Ref. [11]. Authors' data: \circ : [11].

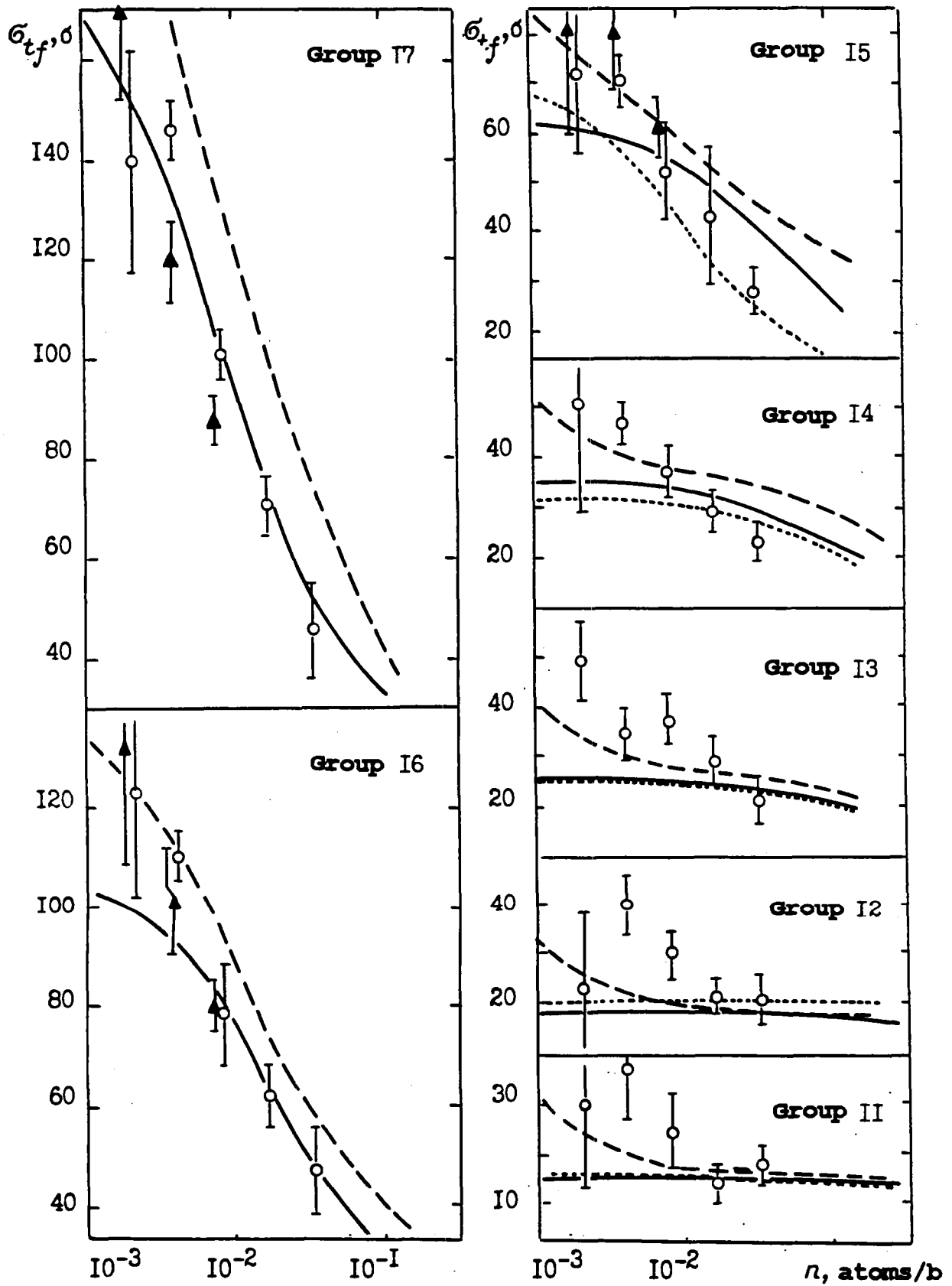


Fig. 8. Comparison of the effective ^{239}Pu cross-section $\sigma_{tf}(n)$ within each energy group.
 Calculation: — using MULTIK; - - - - using BNAB-78;
 using Ref. [11]. Authors' data: ○ : [11]; ▲ - [31].

REFERENCES

1. KOSHCHEEV, V.N, NIKOLAEV, M.N, Voprosy atomnoj nauki i tekhniki. Ser. Yadernye Konstanty, Issue 5 (59) (1984) 16 [in Russian].
2. DOLGOV, E.V., KOSHCHEEV, V.N, SINITSA, V.V., Neutron physics: Materials, 1st Intern. Conf. on Neutron Physics, Kiev 14-18 September 1987, Moscow: TsNII Atominform 1 (1988) 382 [in Russian].
3. ABAGYAN, L.P, BAZAZYANTS, N.O., NIKOLAEV, M.N., TSIBULYA, A.M., "Group constants for reactor and shielding calculations", Moscow: Ehnergoizdat (1981) [in Russian].
4. TAKANO, H., et al., JAERI Fast reactor group constants. Version II, Report JAERI-1255 (1978).
5. VAN'KOV, A.A., GOSTEVA, L.S., UKRAINTSEV, V.F., Voprosy atomnoj nauki i tekhniki, Ser. Yadernye Konstanty, Issue 3 (52) (1983) 27 [in Russian].
6. DOLGOV, E.V., SAVOS'KIN, M.M., TSIBULYA, A.M., Ibid., Issue 5 (59) (1984) 49 [in Russian].
7. NIKOLAEV, M.N., FILIPPOV, V.V., BONDARENKO, I.I., Atomnaya Ehnergiya II (1961) 445 [in Russian].
8. SINITSA, V.V., Voprosy atomnoj nauki i tekhniki, Ser. Yadernye Konstanty, Issue 5 (59) (1984), 34 [in Russian].
9. NIKOLAEV, M.N., BAZAZYANTS, N.O., GORBACHEVA, L.V., et al., Neutron data for uranium-238, Part 2: Preprint OB-70, Obninsk (1979) [in Russian].
10. VAN'KOV, A.A., GRIGORIEV, Yu.V., UKRAINTSEV, V.F., et al., Voprosy atomnoj nauki i tekhniki, Ser. Yadernye Konstanty, Issue 4 (35) (1979) 48 [in Russian].
11. VAN'KOV, A.A., GRIGOR'EV, Yu.V., UKRAINTSEV, V.F., et al., Ibid., Issue 2 (37) (1980) 44 [in Russian].
12. VANKOV, A.A., GRIGORIEV, Yu.V., NIKOLAEV, M.N., et al., Temperature dependence of the cross-section structure of ^{238}U in the unresolved region, Report INDC(CCP)-16/L (1971).
13. FILIPPOV, V.V., Voprosy atomnoj nauki i tekhniki, Ser. Yadernye Konstanty, Issue 4 (1985) 33 [in Russian].
14. KONONOV, V.N., POLETAEV, E.D., In: Neutron physics: Materials. 2nd All-Union Conference on Neutron Physics, Kiev, 28 May-1 July 1973, Obninsk, 2 (1974) 199 [in Russian].
15. BOKHOVKO, M.V., KONONOV, V.N., MANTUROV, G.N., et al., Voprosy atomnoj nauki i tekhniki, Ser. Yadernye Konstanty, Issue 3 (1988) 41 [in Russian].
16. GRIGOR'EV, Yu.V., BAKALOV, T., ILCHEV, G., Preprint FEhI-1216, Obninsk (1981) [in Russian].
17. LITVINSKIJ, L.L., VERTEBNYJ, V.P., LIBMAN, V.A., MURZIN, A.V., Atomnaya ehnergiya, Issue 3, 62 (1987) 92 [in Russian].

18. BYOUN, T.Y., et al., Proc. National Topical Meeting on New Developments in Reactor Physics and Shielding, Sep. 12-15, New York, USAEC (1972) 1115.
19. BYOUN, T.Y., et al., EXFOR Data, Entry-10577.
20. POENITZ, W.P., et al., Nucl. Sci. Eng. 78 (1981) 333.
21. TSANG, F.Y., BRUGGER, R.M., Nucl. Sci. Eng. 72 (1979) 55.
22. TSUBONE, I., Nucl. Sci. Eng. 88 (1984) 579.
23. BEE, N.J., in Proc. IAEA Cons. Meeting on U and Pu Isotopes Resonance Parameters, 28 Sep.- 2 Oct 1981, Vienna, Report INDC(NDS)-129/GJ (1982) 182.
24. BRUGGER, R., AMINFAR, H., Ibid. p.271.
25. PEREZ, R.B., et al., Trans. Amer. Nucl. Soc. 44 (1983) 537.
26. FUJITA, Y., KOBAYASHI, K., YAMOMOTO, S., et al., see Ref.2, Vol.2, p.195.
27. KAZAKOV, L.E., KONONOV, V.N., MANTUROV, G.N., et al., Voprosy atomnoj nauki i tekhniki, Ser. Yadernye Konstanty, Issue 3 (1986) 37 [in Russian].
28. ADAMCHUK, Yu.V., BOSKANYAN, M.A., MURADYAN, G.V., STEPANOV, V.A., See Ref 2, Vol.2, p.242 [in Russian].
29. BRAMBLETT, R.L., CZIRR, J.B., Nucl. Sci. Eng. 35 (1969) 350.
30. CZIRR, J.B., Nucl. Sci. Eng. 70 (1979) 307.
31. CZIRR, J.B., BRAMBLETT, R.L., Nucl. Sci. Eng. 28 (1967) 62.
32. KON'SHIN, V.A., ANTSIPOV, G.V., SUKHOVITSKIJ, E.Sh., et al., Evaluated uranium-235 constants, Minsk: Nauka i tekhnika (1985) [in Russian].
33. ORLOV, V.V., TROYANOV, M.F., MAMONTOV, V.F., et al., Preprint FehI-306, Obninsk (1972) [in Russian].

Submitted for publication 23 February 1988

**TESTING OF CROSS-SECTION FUNCTIONALS
IN THE UNRESOLVED RESONANCE REGION**

V.N. Koshcheev, A.S. Krivtsov
V.V. Sinitsa, V.F. Ukraintsev

ABSTRACT

The results of a comparison of the GRUCON, MMK and NJOY data processing codes in the treatment of evaluated neutron data in the unresolved resonance region are presented. The sets of average resonance parameters of ^{238}U and ^{239}Pu isotopes, which have been published by Munos-Cobos et al., and Ribon et al., were used in this exercise. Average cross-sections, self-shielding factors and Doppler broadening self-shielding factors are compared with the original results presented by the above-mentioned authors. Conclusions regarding the reliability of the neutron data processing codes are made.

After several rounds of international verification of data processing codes under the auspices of the IAEA [1], the attention of many specialists has been focused on the accuracy of neutron data processing.

Drawing on two publications [2, 3] which study the reliability of the methods used for the calculation of resonance cross-section self-shielding factors using test sets of ^{238}U and ^{239}U data as an example, the authors tested the neutron data processing codes used in the Soviet Union (GRUKON, MMK and NJOY) on the basis of the tests proposed in those publications. The tests are totally representative and enable conclusions to be drawn about the reliability of the tested codes used to process evaluated neutron data files and to derive group constants for fast-neutron reactor and radiation shielding calculations.

Testing conditions

Test No. 1 : The average ^{238}U resonance parameters in the energy region 2.0347-3.3546 KeV [2] were obtained by averaging the known resolved resonances parameters. Only the s-wave, which gives the maximum contribution in this energy region is studied. The averaging spectrum $\phi(E) = 1/E$.

Test No. 2 : The average ^{238}U resonance parameters at 4.0 KeV [3]. Although the parameters for s-, p- and d-waves are used for the test, the maximum contribution, as in the case of test No. 1, is made by the s-wave. Unlike test No. 1, the error in the averaging over the energy interval is eliminated.

Test No. 3 : The average ^{239}Pu resonance parameters in the energy range 275.36-454.0 eV [2] are obtained by averaging the parameters of the known resolved resonances. The s-wave which excites states for which $J = 0$ and $J = 1$ is studied.

Consequently, there is the additional (in comparison with tests nos 1 and 2) problem of taking into account the comparable contributions of both states to the non-linear cross-section function parameters. Moreover, there are additional complications associated with taking fission into account. The averaging spectrum $\phi(E) = 1/E$. The average resonance parameters for all the tests are listed in Table 1.

The following cross-section function parameters were calculated and compared:

(1) The mean cross-sections $\langle \sigma_x(T) \rangle = \int \phi(E) \sigma_x(T, E) dE / \int \phi(E) dE$;

(2) The cross-section resonance self-shielding factors for partial cross-sections:

$$f_x(\sigma_0, T) = \langle \sigma_x(T) / [\sigma_t(T) + \sigma_0] \rangle : \{ \langle \sigma_x(T) \rangle \langle 1 / [\sigma_t(t) + \sigma_0] \rangle \},$$

for the total cross-section

$$f_t(\sigma_0, T) = \langle 1 / \sigma_t(T) \rangle \{ \langle 1 / [\sigma_t(T) + \sigma_0] \rangle / \langle 1 / [\sigma_t(T) + \sigma_0]^2 \rangle - \sigma_0 \};$$

(3) The Doppler broadening of the self-shielding factors

$$f_x(\sigma_0, T_2) - f_x(\sigma_0, T_1), \text{ where } x \text{ is the reaction index}$$

t is the temperature of the medium and σ_0 is the dilution cross-section of the nuclide in the medium.

Testing codes

All the codes used in the testing provide various resonance cross-section structure models for calculating function parameters of these cross-sections in the unresolved resonance region. Let us briefly review the characteristics of the calculation models used in the programs.

The GRUKON program [4]

The characteristics of the physical model used to calculate the cross-section function parameters is as follows:

- It is assumed that the reaction cross-section in the vicinity of a given energy point E (comparable to the characteristic dimension of the resonance - the average distance between levels D) can be divided into two components:
 $\sigma(E) = \sigma_R(E) + \sigma_F(E)$, where $\sigma_R(E)$ is the cross-section for the resonance in the vicinity of point E (i.e. resonance cross-section) and $\sigma_F(E)$ is the contribution of all the remaining resonances lying in the vicinity (i.e. smooth cross-section);
- The effect of fluctuations in the resonance and in the smooth cross-section region for a given function parameter are different, the fluctuations of the smooth component $\sigma_F(E)$ are significantly smaller and can be disregarded, i.e. $\overline{F[\sigma_R(E) + \sigma_F(E)]} = \overline{F[\sigma_R(E) + \sigma_F(E)]}$. For linear function parameters this assumption is accurate;
- The resonance component is calculated using the Breit-Wigner formula (single- or multi-level, in the latter case the

interference terms are evaluated from the model of identical equidistant resonances);

- The effect of Doppler broadening of the resonances is calculated with the aid of the ψ and χ resonance form functions;
- The integrals for the resonance width distributions are calculated from quadratic formulas which have a very high degree of algebraic accuracy;
- In order to take account of fluctuations in the resonance width the χ^2_ν distribution is used for ν degrees of freedom. Fluctuations in the gaps between the resonances in the test calculation were not taken into account;
- The cross-sections belonging to different level systems are considered to be statistically independent and therefore the function parameters are initially obtained for each level system separately. Then, for each level system the Pade approximation is performed on the dependence of the function parameter of the dilution cross-section for each isotope in the medium. This makes it possible to determine the subgroup parameters describing the cross-section structure for the given level system. Finally, a convolution of the contributions of all the subgroups of all the level systems in the calculated function parameters is performed.

The MMK Program [5]

In this program the calculation of cross-section function parameters $F(\sigma)$ is based on modelling the cross-section energy dependence (using the "Leder" method). From the physical point of view the MMK program produces the most accurate cross-section calculation model in the unresolved resonance region:

- The parameters of the individual resonances are obtained by selection from the sequence of pseudorandom numbers which follow the Porter-Thomas distribution for the resonance widths and the Wigner distribution for distances between the resonances;

- The detailed energy structure of the cross-section is reproduced either in the Reich-Moore approximation (for fissile nuclei) or the single-level Breit-Wigner approximation (for non-fissile nuclei);
- Analytical account is taken of resonance Doppler broadening, when using the Breit-Wigner approximation account is taken care of by using the form function $\psi-\chi$, in the case of the Reich-Moore approximation, account of the change in the interaction energy as a result of thermal movement is modelled by using pseudo-random numbers weighted by the Maxwellian distribution;
- The cross-section function parameters $F(\sigma)$ are calculated at various temperatures using the same selection of resonances. This ensures acceptable accuracy in the calculation of the Doppler broadening of the resonance self-shielding factors without involving a vast amount of statistics;
- All the function parameters in the program are calculated using the total cross-section probability density function $p(\sigma_t)$ and the correlation function between the partial and total cross-sections $\sigma_x(\sigma_t)$.

The NJOY Program [6]

In this program, the following considerations are taken into account in the calculation of the cross-section function parameters in the unresolved resonance region:

- implementation of the analytical method to calculate the cross-section function parameters for Breit-Wigner resonances;
- calculation of integrals of the function parameters with respect to the resonance width distributions, and of the distances between resonances using quadratic formulas.

At present, the authors do not have a detailed description of the method adopted in the current version of the NJOY program.

There is evidently no correlation between calculation errors using this program and the GRUKON and MMK programs, it is therefore interesting to compare the calculation results obtained using these programs.

Analysis of Results

The calculation results for the average cross-sections and self-shielding factors for the above three tests were compared with original data provided by Muños-Cobos, et al. [3] and Ribon, et al. [2]. The results of the comparison in the form of relative errors of the original data for a set of dilution cross-sections for an isotope, equal to 1, 10, 100 and 100 barns, are shown in tables 2-4. From the data given in the tables, it follows that:

- All the tested programs reproduced the average cross-sections with an acceptable degree of accuracy, with the possible exception of the MMK program in which the statistics need to be improved in order to obtain more accurate results;
- The programs do not reproduce the cross-section self-shielding factors equally well. Particularly marked differences in the self-shielding factors are observed when the dilution cross-section of the isotope in the medium is small (on the order of 1 b). Here, a significant role is played by the extent to which the physical model set up to calculate the cross-section function parameters describes the minima in the total cross-section. By "contaminating" these minima with the background cross-section - the isotope dilution cross-section in the medium, σ_0 , the calculation results become more compatible;
- For the fissile nucleus ^{239}Pu , the self-shielding factors calculations results agree less well than for the non-fissile ^{238}U nucleus. This is particularly manifest in the calculation results for the capture cross-section self-shielding factors, the discrepancies of which reach $\pm 12\%$ for $\sigma_0 = 1$ b in the case of ^{239}Pu .

Tables 5-7 show absolute values for Doppler broadening in the self-shielding factors for the three tests respectively. For the purposes of comparison, the original data were used where available [2 and 3]. It can be seen that, as in the case of the self-shielding factors, the results of calculating the Doppler broadening agree well among themselves in the case of large dilution cross-sections of the isotope in the medium and differ for small (on the order of 1 barn) dilution cross-sections. The greatest differences are observed for Doppler broadening of the self-shielding factors of the total cross-section which confirms the importance of correct reproduction of the minima in the total cross-section. The calculational results for Doppler broadening for those programs which implement the "Leder" method agree among themselves; in the case of the GRUKON program, the results are somewhat higher than for the other programs, and in the case of the NJOY program, lower than the main set of results (with the exception of the capture data). The calculation results of the Doppler broadening of self-shielding factors for the whole set of dilution cross-sections for the non-fissile ^{238}U nucleus agree better than for the fissile ^{239}Pu nucleus.

The set of average resonance parameters examined in this paper relate to the lower part of the unresolved resonance region, in which the effects of cross-section resonance self-shielding and the dependence on temperature is most pronounced. As the energy increases, the effect of overlapping of individual resonances and the contribution of higher waves bring the resonance self-shielding factors closer to unity and their Doppler broadening closer to zero. This gives reason to hope that the tests used in this paper give a clearly enough indication of the accuracies of the methods and programs examined over the whole range of their practical application.

Comparison of the results from the three programs shows that:

1. All programs give reasonably compatible calculation results for the preparation of group constant which are of practical

importance i.e. when the dilution cross-section of the isotope in the medium is large;

2. In the preparation of group constants, the use of programs which use analytical methods for the calculation of cross-section functions, are more rapid in comparison to the more detailed "Leder" method.

Table 1

Average resonance parameters of the tested sets

Test No.	Isotope	AWR	R, fm	ℓ	J	\bar{D} , eV	$\bar{\Gamma}_n^0$, eV	$\bar{\Gamma}_g$, eV	$\bar{\Gamma}_f$, eV	ν_n	ν_f
1	^{238}U	236,006	9,184	0	0,5	20,0	2,2E-3	0,0235	0,0	1	0
2	^{238}U	236,006	9,3981*	0	0,5	20,0	2,10E-3	0,0235	0,0	1	0
				1	0,5	20,0	1,549E-3	0,0235	0,0	1	0
				1,5	10,0	7,745E-4	0,0235	0,0	1	0	
				2	1,5	10,0	2,50E-3	0,0235	0,0	1	0
3	^{239}Pu	236,499	9,0535	0	0,0	8,20	8,49E-4	0,0407	2,495	1	2
					1,0	2,86	2,83E-4	0,0462	0,038	1	1

In the original text of Ref. [3] the value of R = 8.9 fm is given and the background scattering cross-section is used. In Ref. [2] the background scattering cross-section is taken into account by means of the scattering radius R = 9.3981 fm. In this paper, the background scattering cross-section is taken into account in a similar manner.

Table 2

Relative deviations in the average cross-sections and self-shielding factors f from data in Ref. [2] for Test No. 1 (T = 300°K)

Cross-section	Data from Ref [2]		relative deviations		
	f	ϵ , %	MMK	NJOY	GRUKON
σ_0	Elastic scattering				
10^3	0,9501	$\pm 0,1$	+0,4 \pm 0,5	+0,1	+0,1
10^2	0,7970	$\pm 0,3$	+0,8 \pm 1,7	+0,9	+0,3
10^1	0,6504	$\pm 0,5$	+0,7 \pm 2,9	+5,2	+1,2
10^0	0,5879	$\pm 0,6$	-0,1 \pm 4,1	+11,7	+2,7
$\langle \sigma_E \rangle$	18,23	$\pm 0,7$	-1,2 \pm 3,1	+0,9	-0,3
σ_0	Capture				
10^3	0,9402	$\pm 0,1$	-0,1 \pm 0,3	-0,2	0,0
10^2	0,7046	$\pm 0,3$	-0,8 \pm 1,2	-0,8	+0,1
10^1	0,4118	$\pm 0,4$	-1,1 \pm 2,0	+0,3	+0,8
10^0	0,3166	$\pm 0,4$	-1,1 \pm 2,5	+3,4	+2,0
$\langle \sigma_c \rangle$	1,095	$\pm 0,6$	-4,6 \pm 2,4	+1,6	+0,6

Table 3

Relative deviations in the average cross-sections and self-shielding factors f from data in Ref. [3] for Test No. 2 ($T = 300^\circ\text{K}$)

Cross-section	Data from Ref [3]		relative deviations			
	f	$\epsilon, \%$	MMK	NJOY	GRUKON	Data from Ref. [2]
$\langle \sigma_0 \rangle$	Total interaction					
10^2	0,79	$\pm 1,3$	$+2,5 \pm 3,8$	+1,0	+0,1	-
10^1	0,645	$\pm 1,4$	$+3,4 \pm 6,7$	+6,8	+1,1	-
10^0	0,55	$\pm 1,8$	$+7,6 \pm 10,9$	+21,3	+4,2	-
$\langle \sigma_t \rangle$	17,95	-	$-2,2 \pm 5,6$	+0,8	-0,6	$-2,9 \pm 1,2$
σ_0	Capture					
10^2	0,83	$\pm 2,4$	$0,0 \pm 0,8$	+0,4	+0,2	$-0,5 \pm 0,2$
10^1	0,60	$\pm 1,7$	$-0,2 \pm 4,5$	+0,5	+1,7	$-1,0 \pm 1,0$
10^0	0,52	$\pm 1,9$	$-1,3 \pm 5,6$	+0,4	+0,8	$-3,1 \pm 1,6$
$\langle \sigma_c \rangle$	0,926	-	$-0,2 \pm 5,2$	+0,1	-0,1	$-0,8 \pm 1,6$

Table 4

Relative deviations in the average cross-sections and self-shielding factors f from data in Ref. [2] for Test No. 3 ($T = 300^\circ\text{K}$)

Cross-section	Data from Ref [2]		relative deviations		
	f	$\epsilon, \%$	MMK	NJOY	GRUKON
σ_0	Elastic scattering				
10^3	0,9713	$\pm 0,2$	$+0,1 \pm 0,3$	+0,1	+0,1
10^2	0,8911	$\pm 0,4$	$+0,3 \pm 1,0$	+0,3	+0,4
10^1	0,8255	$\pm 0,6$	$+0,4 \pm 1,5$	+0,5	+0,9
10^0	0,8079	$\pm 0,6$	$+0,2 \pm 1,6$	+0,7	+1,4
σ_E	13,30	+0,8	$+3,0 \pm 1,8$	+0,5	+0,1
σ_0	Fission				
10^3	0,9541	$\pm 0,2$	$0,0 \pm 0,3$	+0,1	-0,2
10^2	0,7795	$\pm 0,6$	$-0,4 \pm 1,3$	+0,3	-0,1
10^1	0,5592	$\pm 1,1$	$-1,7 \pm 2,3$	-1,7	+2,3
10^0	0,4865	$\pm 1,2$	$-2,7 \pm 2,6$	-5,5	+4,6
$\langle \sigma_E \rangle$	9,57	$\pm 1,5$	$-1,9 \pm 7,2$	-0,8	-0,3
σ_0	Capture				
10^3	0,9228	$\pm 0,2$	$-0,5 \pm 0,4$	+0,1	-0,1
10^2	0,6587	$\pm 0,5$	$-2,4 \pm 1,4$	-0,2	+1,7
10^1	0,3890	$\pm 0,8$	$-4,7 \pm 2,1$	-5,9	+7,4
10^0	0,3147	$\pm 0,9$	$-5,5 \pm 2,4$	-12,9	+11,6
$\langle \sigma_c \rangle$	9,38	$\pm 1,0$	$-0,5 \pm 4,2$	+0,4	-0,2

Table 5

Doppler broadening of self-shielding factors, calculated from various programs for Test No. 1

Cross-section $\sigma_{0,6}$	MMK	NJOY	GRUKON	MMK	NJOY	GRUKON
	$f_{\pm}(900 \text{ K}) - f_{\pm}(300 \text{ K})$			$f_{\pm}(2100 \text{ K}) - f_{\pm}(900 \text{ K})$		
10^3	0,027	0,028	0,028	0,018	0,018	0,018
10^2	0,049	0,046	0,050	0,044	0,043	0,046
10^1	0,036	0,023	0,038	0,036	0,030	0,041
10^0	0,073	0,016	0,066	0,052	0,023	0,053
	$f_E(900 \text{ K}) - f_E(300 \text{ K})$			$f_E(2100 \text{ K}) - f_E(900 \text{ K})$		
10^3	0,015	0,016	0,016	0,009	0,010	0,010
10^2	0,041	0,039	0,042	0,033	0,033	0,034
10^1	0,038	0,031	0,040	0,037	0,033	0,040
10^0	0,045	0,025	0,045	0,040	0,030	0,043
	$f_c(900 \text{ K}) - f_c(300 \text{ K})$			$f_c(2100 \text{ K}) - f_c(900 \text{ K})$		
10^3	0,023	0,024	0,023	0,013	0,014	0,013
10^2	0,083	0,087	0,085	0,059	0,063	0,062
10^1	0,098	0,107	0,104	0,089	0,099	0,098
10^0	0,086	0,100	0,094	0,089	0,102	0,102

Table 6

Doppler broadening of self-shielding factors, calculated from various programs for Test No. 2

Cross-section	Ref. [3] data	MMK	NJOY	GRUKON	Ref. [3] data	MMK	NJOY	GRUKON	Ref. [2] data
		$f_{\pm}(1000 \text{ K}) - f_{\pm}(300 \text{ K})$				$f_{\pm}(2000 \text{ K}) - f_{\pm}(1000 \text{ K})$			
10^2	0,05	0,046	0,046	0,050	0,03	0,026	0,026	0,031	-
10^1	0,043	0,045	0,030	0,049	0,034	0,032	0,027	0,037	-
10^0	0,072	0,060	0,022	0,077	0,044	0,040	0,021	0,045	-
		$f_c(1000 \text{ K}) - f_c(300 \text{ K})$			$f_c(2000 \text{ K}) - f_c(1000 \text{ K})$			Δf_c^*	
10^2	0,06	0,060	0,064	0,062	0,03	0,029	0,032	0,032	0,088
10^1	0,10	0,095	0,106	0,103	0,06	0,059	0,067	0,067	0,151
10^0	0,10	0,096	0,109	0,109	0,07	0,066	0,076	0,077	0,162

* $\Delta f_c = f_c(2000 \text{ K}) - f_c(300 \text{ K})$.

Table 7

Doppler broadening of self-shielding factors, calculated from various programs for Test No. 3

Cross-section $\sigma_{0.6}$	MMK	NJOY	GRUKON	MMK	NJOY	GRUKON
	$f_t(900 \text{ K}) - f_t(300 \text{ K})$			$f_t(2100 \text{ K}) - f_t(900 \text{ K})$		
10^3	0,029	0,031	0,029	0,017	0,019	0,019
10^2	0,058	0,060	0,065	0,049	0,056	0,058
10^1	0,038	0,010	0,061	0,045	0,011	0,066
10^0	0,030	-0,014	0,062	0,039	-0,016	0,070
	$f_E(900 \text{ K}) - f_E(300 \text{ K})$			$f_E(2100 \text{ K}) - f_E(900 \text{ K})$		
10^3	0,009	0,010	0,009	0,005	0,006	0,008
10^2	0,021	0,024	0,025	0,017	0,020	0,022
10^1	0,019	0,018	0,023	0,019	0,021	0,026
10^0	0,017	0,013	0,022	0,018	0,016	0,026
	$f_F(900 \text{ K}) - f_F(300 \text{ K})$			$f_F(2100 \text{ K}) - f_F(900 \text{ K})$		
10^3	0,014	0,015	0,015	0,009	0,010	0,010
10^2	0,047	0,051	0,051	0,036	0,043	0,042
10^1	0,056	0,050	0,066	0,055	0,055	0,066
10^0	0,054	0,030	0,071	0,058	0,034	0,074
	$f_C(900 \text{ K}) - f_C(300 \text{ K})$			$f_C(2100 \text{ K}) - f_C(900 \text{ K})$		
10^3	0,029	0,031	0,030	0,016	0,018	0,019
10^2	0,089	0,102	0,097	0,063	0,079	0,074
10^1	0,094	0,111	0,120	0,085	0,116	0,109
10^0	0,085	0,090	0,124	0,085	0,102	0,119

REFERENCES

1. CULLEN, D.E., The IAEA cross-section processing code verification project, Report INDC(NDS)-170, IAEA, Vienna (1985).
2. RIBON, P., SAUVINET, V., MOUSSALEM. P., Etudes des methodes de calcul de l'autoprotection dans les resonances, Report CEA-N-2426 (also NEACRP-A-696) (1985) [in French].
3. MUÑOS-COBOS, J.L., DE SAUSSURE, G., PEREZ, R.B., Sensitivity of computed ²³⁸U self-shielding factors to the choice of the unresolved average resonance parameters, Nucl. Sci. Eng. 81 (1982) 55.
4. SINITSA, E.V., Calculation of cross-section self-shielding resonance factors in the unresolved resonance region. Voprosy Atomnoj Nauki I Tekhniki, Ser. Nuclear Constants 5(54) (1983) 54 [in Russian].
5. NEFED'EVA, L.S., UKRAINTSEV, V.F., YANEVA, N., Set of programs for modelling the cross-sections of transactinide nuclei in the unresolved resonance region. OIYAI Report No. P10-86-124 Dubna (1986) [in Russian].
6. MacFARLAND, R.E., BARRET, R.J., MUIR, D.W., BOICOURT, R.M., The NJOY nuclear data processing system: User's Manual, Report LA-7584-M, Los Alamos National Laboratory (1978).

Submitted for publication 30 December 1986.

POSSIBLE INFLUENCE OF CORRELATION BETWEEN ν AND Γ_r ON RESONANCE SHIELDING OF $\bar{\nu}$

A.G. Gusejnov, M.A. Gusejnov, N.S. Rabotnov

ABSTRACT

The effect of a phenomenological positive correlation between the average number of prompt fission neutrons and fission widths on the resonance self-shielding of $\bar{\nu}$ is investigated. Both an estimate of the isolated resonance approximation and direct numerical calculations for $0.2 \text{ eV} \leq E_n \leq 50 \text{ eV}$ in ^{239}Pu show that the increase of $\bar{\nu}$ resulting from self-shielding may be 0.2 to 0.3%.

The dependence on excitation energy of the number of prompt fission neutrons ν averaged over a suitably large number of levels of a fissile nucleus can, with a fair degree of accuracy, be taken to be linear where the neutron energy is high enough to cause fission ($E_n \geq 1 \text{ MeV}$) [1]. There are indications that the value of ν varies even in the resonance region. These variations are of interest both from the point of view of understanding their physical nature, and when one is accounting for their influence on the results of reactor calculations. They may be of two types:

- Random changes from resonance to resonance which show no correlation with other level characteristics (spins J , partial and total widths);
- Systematic changes which do show such a correlation.

Clearly, it may be essential to take into account variations of the first type in the very lowest energy groups but, as the energy and the number of resonances in the group increases, they

should average out. Variations of the second kind may be smaller in amplitude, but they may give rise to a certain dependence on J and $\bar{\Gamma}_1$ values even in averaged values; consequently, cross-section resonance self-shielding may exert an influence on $\bar{\nu}$ which may, in principle, be measured in experiments using filtered beams or in integral experiments.

The results systematized in Ref. [2] indicate that precisely such a systematic effect may exist; they reveal an approximately linear dependence of the value of ν on the inverse of the fission width. This effect is most noticeable for I^+ resonances in ^{239}Pu , and the authors of that paper connected it with the reaction $(n, \gamma f)$; Ref. [3] first indicated the possibility that this reaction might be occurring. This paper evaluates the influence of that correlation on possible "shielding" of $\bar{\nu}$.

Simplest evaluation of the possible magnitude of the effect.

In line with the phenomenological conformity revealed in Ref. [2], let us assume that the number ν is related to the resonance fission width Γ_f in the following way:

$$\nu = \nu_0[(1 - \Delta)/\Gamma_f] \quad [1]$$

Expression (1) must be averaged using the weighting factor proportional to the contribution of the resonance under investigation to the fission cross-section; in the isolated resonance approximation this is the area under the resonance curve. Where there is no shielding it is proportional to $\Gamma_n \Gamma_f / \Gamma$, and where there is shielding it is related to the partial widths in a more complex manner. From this point, averaging over the statistical distributions of the partial widths of resonances with the above-mentioned weighting factor will be indicated by the use of angled brackets. Fluctuations in the fission and reduced neutron widths can be assumed to be independent, and insignificant fluctuations in the radiation width can be ignored and assumed to be constant. In addition, for fissile nucleus

resonances the inequalities $\Gamma_n \ll \Gamma_\gamma$ and $\Gamma_n \ll \Gamma_f$ apply, and the total width may be taken to be approximately equal to the sum of the fission and the radiation widths: $\Gamma = \Gamma_\gamma + \Gamma_f$. The existence of the reaction $(n, \gamma f)$ should cause the fission width to be split into two components: $\Gamma_f = \Gamma_{\gamma f} + \Gamma'_f$, where $\Gamma_{\gamma f}$, like the radiation width, does not fluctuate, and Γ'_f obeys the Porter-Thomas distribution having a mean value of $\bar{\Gamma}'_f$. Thus, averaging expression (1) we obtain:

$$\langle \nu \rangle = \nu_0 \left(1 - \frac{\Delta}{\bar{\Gamma}'_f} \left\langle \frac{1}{x + \beta} \right\rangle \right), \quad (2)$$

where $x = \Gamma'_f / \bar{\Gamma}'_f$, and $\beta = \Gamma_{\gamma f} / \bar{\Gamma}'_f$. Insofar as $\langle x \rangle = 1$, and $\left\langle \frac{1}{x + \beta} \right\rangle \approx 1$ where there is no shielding, one may expect that, as shielding increases, the influence of fluctuation will be mitigated and $\left\langle \frac{1}{x + \beta} \right\rangle$ will approach unity. The actual change is also of the order of 1. Thus, the maximum change (increase) in $\langle \nu \rangle$ due to shielding should correspond to $\Delta / \bar{\Gamma}'_f$. According to the data given in Ref. [2], $\Delta = 0.22$ MeV for the I^+ resonances in ^{239}Pu , and $\bar{\Gamma}'_f = 40$ meV. Therefore the possible change in the number $\langle \nu \rangle$ due to shielding is not greater than 0.5%. This value, if it is realistic, is not small enough to be negligible. Consequently, a more detailed evaluation must be carried out.

Calculation in the isolated resonance approximation.

Let us assume that the dependence of the total cross-section σ_t and the fission cross-section σ_f on energy E_0 near the s-resonance level is described by the single-level Breit-Wigner formula $\sigma_t(E) = \Gamma_n \Gamma_f / [(E - E_0)^2 + (\Gamma/2)^2]$. Here, $a = g \pi \lambda^2$, where λ is the length of the neutron wave; $g = (2J + 1) / 2(2I + 1)$; I and J are the spin of the target nucleus and the resonance respectively. The fission cross-section $\sigma_f = \sigma_t \Gamma_f / \Gamma$. We then determine the area under the resonance of fission cross-section taking shielding into account:

$$\Sigma = \int_{-\infty}^{\infty} dE \exp[-\sigma_t(E) n] \sigma_f(E) = 2\pi a \frac{\Gamma_n \Gamma_f}{\Gamma} \exp(-2an\Gamma_n) I_0(2an\Gamma_n),$$

where $\gamma_n = \Gamma_n/\Gamma$, n is the effective thickness of the absorber in nuclei/ b and I_0 is the Bessel function of the third kind. We then introduce the additional designations $\Gamma_n/\bar{\Gamma}_n = \gamma$, $\Gamma_\gamma/\bar{\Gamma}_\gamma = \alpha$, $c = \alpha + \beta$, $\bar{\Gamma}_n/\bar{\Gamma}_\gamma = \epsilon$ and the Porter-Thomas distribution function (χ^2 is the distribution with the number of degrees of freedom ν)

$$\varphi_\nu(z)dz = \frac{(\nu z/2)^{\nu/2-1} \exp(-\nu z/2) dz}{\Gamma(\nu/2)} \frac{\nu}{2} \quad (3)$$

and from this point we shall assume that the value of γ obeys the distribution given in (3) with the number $\nu = \nu_n = 1$, and that the value of x obeys the same distribution with $\nu = \nu_\gamma = 1$ (or 2). Then the unknown averaged value $\langle 1/(x + \beta) \rangle$ in formula (2) may be expressed in the following form:

$$\langle z \rangle \equiv \left\langle \frac{1}{x+\beta} \right\rangle = I_{\nu_n \nu_\gamma}^0(c, g) / [I_{\nu_n \nu_\gamma}^1(c, g) + \beta I_{\nu_n \nu_\gamma}^0(c, g)], \quad (4)$$

where $g = 2\alpha n \epsilon$, and the integrals

$$I_{\nu \mu}^l(c, g) = \int_0^\infty \int_0^\infty dx dy \varphi_\nu(y) \varphi_\mu(x) \frac{\epsilon y x^l}{x+c} \exp[-gy/(x+c)] I_0[gy/(x+c)]. \quad (5)$$

Expression 5, by integration with respect to y , is converted into a single integral which takes the form

$$I_{11}^l(c, g) \sim \int_0^\infty \frac{dx \exp(-x/2) x^l E(k)}{\sqrt{x(x+c)(x+c+4g)}} \quad \text{при } \nu_\gamma = 1; \quad (6)$$

$$I_{12}^l(c, g) \sim \int_0^\infty \frac{dx \exp(-x) x^l E(k)}{\sqrt{(x+c)(x+c+4g)}} \quad \text{при } \nu_\gamma = 2, \quad (6')$$

where $E(k)$ is the total elliptic integral $k = \sqrt{4g/(x+c+4g)}$. Certain general multipliers which do not depend on the index l and are therefore abbreviated in expression (4), have been omitted from these expressions, and the equality signs have been replaced by the proportionality sign.

First of all let us compute the expressions (6)-(6') for the extreme cases of absorber thickness $g = 0$ and $g \rightarrow \infty$. In the

first instance, $K = 0$ and $E(0) = \pi/2$, and in the second, $K = 1$ and $E(1) = 1$. Direct integration and substitution into expression (4) yields:

for $g = 0$ (7)

$$\langle z \rangle = \left[\sqrt{\frac{2c}{\pi}} \frac{\exp(-c/2)}{\operatorname{erfc}(\sqrt{c}/2)} - c + \beta \right]^{-1}, \quad \nu_f = 1;$$

$$\langle z \rangle = -Ei(-c) / [\exp(-c) + (c - \beta)Ei(-c)], \quad \nu_f = 2; \quad (7')$$

for $g = \infty$ (8)

$$\lim \langle z \rangle = \frac{2}{c} \left[\frac{K_1(c/4)}{K_0(c/4)} - 1 \right]^{-1}, \quad \nu_f = 1;$$

$$\lim \langle z \rangle = \left[\frac{\Gamma(3/2, c)}{\Gamma(1/2, c)} - c \right]^{-1}, \quad \nu_f = 2, \quad (8')$$

where $\Gamma(a, x)$ is the incomplete γ -function; $K_1(x)$ is the Macdonald function; $E_1(x)$ is the integral exponent [$E_1(-x) < 0$]. Assuming monotonic dependence of the effect on g , its maximum value takes the form of the difference

$$\Delta r = \langle r(g = 0) \rangle - \langle r(g = \infty) \rangle.$$

The behaviour of $\Delta r(c)$ is shown by the curves in Fig. 1.

For arbitrary values of g the integrals (6)-(6') should be solved numerically. Examples of the $r(c, g, \beta)$ dependences obtained are given in Fig. 2 for parameter values in the ranges $0.2 \leq c \leq 1$, $0 \leq g \leq 1.5$ and $0 \leq \beta \leq 2$. In reality, values for c and g change within these limits. The evaluation of the size of $\beta = \Gamma_{\gamma f} / \bar{\Gamma}_f$ is suitably indeterminate [2, 4]. The non-fluctuating value $\Gamma_{\gamma f}$ should not exceed the minimum observable values of Γ_f which, for fissile nuclei, comprise a few meV. The resulting values for β are deliberately confined to the range given above - $\beta \leq 0.2$.

Discussion of results.

Let us discuss the results obtained for the ^{239}Pu nucleus for which one can expect a maximum value for the effect owing to the following characteristics:

- Largest observable value for the coefficient $\Delta/\bar{\Gamma}_r$ in expression (1) for the I^+ resonance spin subsystem;
- Largest average distance between resonances by comparison with the other fissile nuclei ^{235}U and ^{233}U , and pronounced resonance structure which magnifies shielding effects.

Although the resonance structure of ^{239}Pu cross-sections has been analysed up to approximately 500 eV, the most reliable data on average widths and cross-sections for the two spin subsystems are concentrated in the range up to 200 eV. At higher energies, level suppression becomes more frequent and the problems of identifying resonances from spin are greater. Let us examine the range up to 200 eV. The data required for the evaluations are given in the table. The boundaries of the energy ranges in the majority of cases are the same as the group boundaries in the 26-group constant system. There are only three resonances below 10 eV, and an evaluation using statistical methods is clearly inapplicable here.

The average widths are calculated from evaluated data in [5], and the average cross-section values were computed using the GRUKON program package [6], also using evaluated data. The small value for the constant $\Delta/\bar{\Gamma}_r$ in expression (2) for 0^+ resonances (it is at least an order smaller than for I^+), their very large average fission width and consequently, their small cross-section value at the maximum points lead one to assume that there must be no shielding of $\bar{\nu}$ at all for this spin subsystem, and shielding of the cross-sections is noticeably lower. Therefore, one can only expect to see the effect in those groups where the

contribution of I^+ resonances to the total fission cross-section is predominant. As may be seen from the table, there are two such groups: 10-21.5 eV and 21.5-46.5 eV. The $\bar{\sigma}_f^+ / \bar{\sigma}_f^{0+}$ ratio in these ranges is 6.7 and 6.0 respectively. Within the accuracy limits of our evaluation, contribution of 0^+ levels could be ignored. In the other groups this ratio is approximately equal to or less than one and should decrease as resonance self-shielding increases, so the effect of $\bar{\nu}$ shielding in these groups can be assumed to be small.

The radiation width is approximately constant and is equal to 43 meV [5], and for the unified group 10-46.5 meV $\bar{\Gamma}_f = 42$ meV (see Table). Thus, a value of $c = 1$ should be chosen for the formulae given above. Despite the indeterminacy noted in the value of $\Gamma_{\gamma f}$, it is clear that this value makes up only a small portion of $\bar{\Gamma}_f$ and therefore, for evaluation purposes, one can assume $\beta = 0$. In line with the results shown in Fig. 1, where $c = 1$ and $\nu_f = 1$, when $\bar{\nu}$ shielding reaches saturation, $\Delta r = 0.5$ and the corresponding relative increase in the number ν is approximately $0.5\Delta/\bar{\Gamma}_f = 0.25\%$.

The approximation of isolated resonances used is fairly rough. Therefore, in order to make the evaluation more accurate, a numerical calculation can be made taking into account the real resonance structure while preserving the basic assumption that the correlation of ν with the fission width of the resonance is described by expression (1).

Numerical calculation using evaluated resonance parameters.

Since the isolated resonance approximation used above is fairly crude, it was decided to carry out a direct numerical calculation of the number $\langle \nu \rangle$ for several absorber thicknesses using detailed information on the fission cross-section and the total cross-section for ^{239}Pu in the resonance region. In this case

$$\langle \nu \rangle = \frac{\int_{E_{\min}}^{E_{\max}} dE \phi(E) \sum_{i=1}^N \nu_i \sigma_{fi}(E) \exp \left[-tn \sum_{i=1}^N \sigma_{ti}(E) \right]}{\int_{E_{\min}}^{E_{\max}} dE \phi(E) \sum_{i=1}^N \sigma_{fi}(E) \exp \left[-tn \sum_{i=1}^N \sigma_{ti}(E) \right]}, \quad (9)$$

where $\phi(E)$ is the spectrum of the neutrons incident upon the absorber; the index i numbers the resonances, and the contribution of each resonance to the cross-section is determined from its Adler-Adler formalism parameters:

$$\sigma_{fi}(E) = \frac{1}{\sqrt{E}} \frac{A_{fi}(E - \epsilon_i) + B_{fi}}{(E - \epsilon_i)^2 + G_i^2} \quad (10)$$

and for the total cross-section, in a similar manner to the other parameters A_{ti} and B_{ti} . The value for the number of prompt fission neutrons over the given resonance was determined, as before, using the expression $\nu_i = \nu^J_0 (1 - \Delta^J / \Gamma_{tc})$. The values ν^J_0 and Δ^J , according to the data in Ref. [2], are almost independent of the spin J : $\nu^1_0 = 2.87$; $\nu^0_0 = 2.88$; $\Delta^1 \nu^1_0 = 0.7$ meV; $\Delta^0 \nu^0_0 = 0.74$ meV (however, one should not forget that the effect is determined using the indefinite quantity $\Delta^J / \bar{\Gamma}_{tc}$, and it is approximately 50 times smaller for $J = 0$ than for $J = 1$). The parameters A , B , ϵ and G in expression (10) were taken from the evaluation in Ref. [7] which describes most accurately the behaviour of ^{239}Pu cross-sections in the resonance region. The total number of terms in the summations in expression (9) is $N = 217$. The energy interval $E_{\min} = 0.2$ eV, $E_{\max} = 50$ eV was looked at, the Fermi spectrum $\phi(E) = 1/E$ was chosen for the neutron spectrum, and the density of the absorber n was taken to be $0.504 \times 10^{23}/\text{cm}^3$.

From the computational point of view, one should also note one significant difference between the evaluation using formula (2) and calculations using expression (9). In formula (2) the effect is presented in the form of a small term where the value of the coefficient must be evaluated; this does not require a high level of accuracy in the calculation. In expression (9), on the other hand, to find the weak

dependence $\langle \nu \rangle(t)$ the integrals from highly complex functions must be computed to a high degree of accuracy. For absorber thicknesses t of 0.05, 0.1, 0.15 and 0.6 cm, the following values were obtained for the effect: 0.19, 0.26, 0.29 and 0.38% respectively, showing a qualitative agreement with the evaluation given in Refs [2-4].

The evaluations performed yield a small value - approximately 0.2-0.3% - and the shielding effect of the $\bar{\nu}$ value is concentrated in the low energy groups of the resonance region. It is hardly noticeable in experiments with filtered beams and in integral experiments. However, just recently data have appeared (see Ref.[8] and the reference materials used in that paper) concerning possible existence of a systematic difference of approximately 2% in the mean values for the number $\bar{\nu}$ for the 0^+ and I^+ resonances in ^{239}Pu . If this is substantiated, the ν shielding effect should increase close to 1% assuming the figure does not change. We feel that further calculations should be done, and that possible influence on the temperature effect in reactors should be looked at

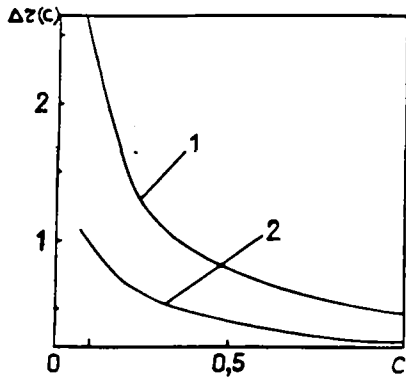


Fig. 1. Dependence of $\Delta r = r(0) - r(\infty)$ on c for v_i equal to 1 and 2 (curves 1 and 2 respectively).

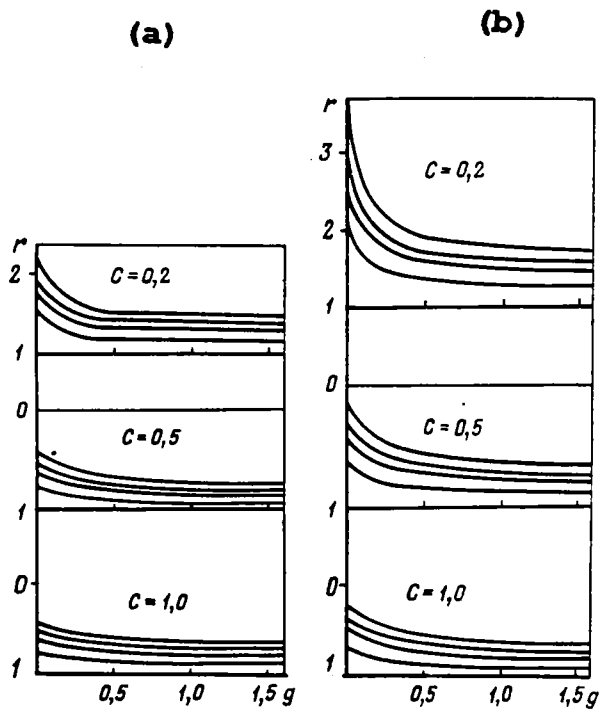


Fig. 2. The dependence $r(v_i, c, g, \xi)$ determined by using expressions (4)-(6): (a) - $v_i=2$; (b) - $v_i=1$. For each set of 4 curves the values of ξ are 0, 0.05, 0.1, 0.2 (top to bottom).

Table
Data on the mean characteristics of the 0^+ and 1^+
resonance subsystems for ^{239}Pu

Average characteristics	$E_{\min} - E_{\max}$, eV			
	10 - 21.5	21.5 - 46.5	46.5 - 100	100 - 200
$\Gamma_f^{1^+}$, meV	55	29	43	29
$\sigma_f^{1^+}$, barns	73.1	14.9	25.3	7.7
$\Gamma_f^{0^+}$, meV	650	112	1970	1030
$\sigma_f^{0^+}$, barns	10.9	2.5	33.8	11.7

Note: E_{\min} and E_{\max} are the boundaries of the energy range investigated .

REFERENCES

1. GANGRSKIJ, Yu.P., DALKHSUREHN, B., MARKOV, B.N., Fission fragments from nuclear fission, Ehnergoatomizdat, Moscow (1986) 105. [in Russian]
2. TROCHON, J. La réaction $(n, \gamma f)$ dans les résonances induites par neutrons lents dans ^{239}Pu , ^{235}U , ^{241}Pu - (in Proc. 4th IAEA Symp. on Physics and Chemistry of Fission, Julich) 1 (1979) 87 [in French].
3. STAVINSKY, V.S., SHAKER, M.O., The $(n, \gamma f)$ -process, Nucl. Phys., 62 (1965) 667.
4. RYABOV, Yu., TROCHON, J., SHACKLETON, D. Experimental evidence for the $(n, \gamma f)$ -reaction, Gamma ray multiplicity in ^{239}Pu fission induced by neutrons, *ibid.* A216 (1973) 395.
5. ANTSIPOV, G.V., BAKHANOVICH, L.A., ZHARKOV, V.F. et al., Evaluation of nuclear data for ^{239}Pu , Part 1: Resolved resonance region 10^{-5} -660 eV, Preprint 12 ITM AN BSSR [Byelorussian Academy of Sciences Institute of Heat and Mass Transfer] Minsk (1981). [in Russian]
6. SINITSA, V.V., The GRUKON Package, Preprint FEhI-1188, Obninsk (1981) [in Russian].
7. KOLESOV, V.V., LUK'YANOV, A.A., Parameters for multigroup analysis of ^{239}Pu cross-sections in the resonance region, Preprint FEhI-1404, Obninsk (1983). [in Russian]
8. WALSH, R.L., BOLDEMAN, J.W., Spin dependence of ν_p and E_k for ^{239}Pu (n, f) in the resonance region, Nucl. Phys. A451 (1986) 113.

Submitted for publication 26 January 1987.